EFFECTS OF NANOSTRUCTURED MATERIALS ON BACTERIA

A Thesis

by

BRADY M REED

Submitted to the Office of Graduate and Professional Studies of
Texas A&M University
in partial fulfillment of the requirements for the degree of

MASTER OF SCIENCE

Chair of Committee,	Hong Liang
Co-Chair of Committee,	Z.J. Pei
Committee Members,	Jeffrey Cirillo
	Sevan Goenezen
Head of Department,	Andreas A. Polycarpou

December 2018

Major Subject: Mechanical Engineering

ABSTRACT

Nanoparticles and nanostructured materials have attracted great interest for treating bacteria as a potential chemical-free method. This research carries out experiments to evaluate the antibacterial properties of nanoparticles and nanostructured materials. The commonly found bacterium *Staphylococcus aureus* was chosen for this study because of the extensive research and development surrounding the bacteria, its importance in human disease, and its extensive antibiotic resistance, particularly with methicillin-resistant *S. aureus* (MRSA) strains. The specific strain *S. aureus* Xen36 was selected due to its property of bioluminescence, which allows for real-time monitoring of the bacterial loads. Materials investigated were fabricated as particles and deposited on metallic substrates. Substrate materials of copper, aluminum, steel, and nickel were chosen because of their wide applications in manufacturing, particularly in the oil/gas industry.

Results involving nanoparticles showed that V_2O_5 nanoparticles have potential antibacterial effects on *S. aureus*. They are effective in reducing the bacterial load after 2 and 24-hours of treatment. A decrease in bacterial load of 92.4%, 96.7%, and 94.3% was observed when cultured with the V_2O_5 nanoparticles at a concentration of 500ug/mL for 24 hours (NP concentration and incubation time), 1mg/mL for 2 hours, and 1mg/mL for 24 hours, respectively.

Results involving nanostructured materials, i.e., nanoparticle V_2O_5 grown on nickel substrate. These materials cause a 99.1% decrease in bacterial load compared to a control over a 24-hour period.

This research suggests that the effectiveness using a V_2O_5 nanoparticles deposited on a nickel substrate has the potential to be used for control and elimination of bacterial growth. A physical mechanism is proposed to explain these effects.

DEDICATION

To my parents, for teaching me that strong integrity and work ethic is of the utmost importance.

To my Papa and Nana, for always instilling in me a love of learning.

ACKNOWLEDGEMENTS

I would like to thank Dr. Hong Liang for her support and guidance through this process.

Dr. ZJ Pei for his advice and guidance on the applications for this research, as well as the funding from the Industrial & Systems Engineering Department for this project.

Dr. Jeffrey Cirillo for his advice and help in developing the protocol for the nanostructure experiments at the Health Science Center (HSC). His guidance was instrumental in getting the experiments up and running and completing the testing in a timely manner.

Dr. Preeti Sule and Dr. Riti Sharan for their help and advice for the bacterial experiments at the Health Science Center.

Toriq Mustapha for his assistance during the nanoparticle experiments at the Health Science Center.

Dr. Sevan Goenezen for his advice and willingness to be on my graduate committee.

Dr. Jun Qu (Oak Ridge National Laboratory) for providing an internship opportunity for me to learn about materials and characterization, and his advice and access to surface analysis and microscopy equipment.

Other students from the Surface Science research group for their help in training and materials advice: Dr. (Jonny) Yuan Yue, Dr. Yunyun Chen, Eugene Chen, Lian Ma, Kyungjun Lee, and Yan Chen

CONTRIBUTORS AND FUNDING SOURCES

The research discussed in this thesis consists of collaborative research between the Texas A&M University Departments of Mechanical Engineering (MEEN), Materials Science and Engineering (MSEN), and Industrial and Systems Engineering (ISEN), as well as the Texas A&M University Health Sciences Center (HSC) Department of Microbial Pathogenesis and Immunology (MPIM).

Contributors

This work was conceived and directed by Professor Liang and supervised by a thesis committee consisting of Professor Hong Liang (advisor) of the Department of Mechanical Engineering, Professor ZJ Pei of the Department of Industrial and Systems Engineering, and Professor Jeffrey Cirillo of the Department of Microbial Pathogenesis and Immunology, Health Science Center. Support in material characterization was partially provided by Dr. Jun Qu at ORNL.

The Y_2O_3 and ZrP nanoparticles were fabricated by Yunyun Chen, Ph.D. of the Department of Materials Science and Engineering. The V_2O_5 nanoparticles were fabricated by Yuan Yue, Ph.D. of the Department of Materials Science and Engineering. Yuan Yue also fabricated and developed the fabrication method for Ni/Ni-porous/V2O5 nanocomposites used in Chapters 4 and 6. Lian Ma (Ph.D. student) assisted in the electrodeposition process described in Chapters 4 and the optical microscopy and SEM imaging of bacteria in Chapter 6. Eugene Chen (Ph.D. student) of the Department of Materials Science and Engineering assisted in the surface morphology in Chapter 4. Kyungjun Lee (Ph.D. student) of the Department of Mechanical Engineering assisted in the SEM imaging in chapter 4.

Toriq Mustapha (graduate student) of the Department of the Texas A&M University Department of Biology and the Health Science Center assisted with the bacteria

– nanoparticle experiment described in Chapter 5. Dr. Riti Sharan and Dr. Preeti Sule of the Department of Microbial Pathogenesis and Immunology (Health Science Center) assisted in the nanoparticle and nanostructure experiments in Chapters 5 and 6.

All other work conducted for this thesis was completed by the student independently.

Funding Sources

This research was sponsored by Texas A&M Strategic Seed Grant (T3) program, GE Water and Technology, STLE Houston Scholarship program, the startup fund of Dr. Z.J. Pei from the Department of Industrial and Systems Engineering, and in part by an appointment to the Science Education and Workforce Development Programs at Oak Ridge National Laboratory, administered by ORISE through the U.S. Department of Energy Oak Ridge Institute for Science and Education, under Dr. Jun Qu.

NOMENCLATURE

NP	Nanoparticle
SEM	Scanning electron microscope
CFU	Colony forming unit
MWF	Metalworking fluid
HSC	Health Science Center
BCC	Body-Centered-Cubic
FCC	Face-Centered-Cubic

TABLE OF CONTENTS

Page

LIST OF FIGURES

LIST OF TABLES

Page

CHAPTER I

INTRODUCTION

The research in this thesis studies the potential antibacterial effects of a few selected nanomaterials. This chapter provides background information by giving a topical review, discussing *Current Treatment of Bacteria with Nanomaterials*. It provides a brief overview into current antibacterial nanomaterials, with an emphasis on physical and morphological-based treatments of bacteria. Mechanisms of attack and the potential for reusable nanomaterial treatments is also examined. The review helps to set a foundation for this research on potential treatment methods.

1.1 Current Treatment of Bacteria with Nanomaterials

Nanomaterials are of great research interest in many fields owing to their unique properties compared to bulk materials. High surface area-to-volume ratios, Numerous nanomaterials have been proven to have antibacterial effects including silver, copper, carbon (graphite and graphene forms), and many metal oxides (notably zinc oxide). Applications include dental, textiles, paper, water treatment, wound dressing, surgical masks. Research has shown that the morphology of the nanomaterials is extremely important for the overall effectiveness and mechanism of treatment. Silver is the most commonly studied and most widely known antibacterial nanomaterial. Copper, metal oxides (particularly zinc oxide), and various carbon-based nanomaterials, including graphite and graphene, have also been shown to have wide-ranging antibacterial effects.

Material	Pros	Cons	Mechanisms	Applications
Silver	Extremely effective, multiple mechanisms, large	More expensive, toxicity in humans	Inhibition of intracellular activity, incorporation into cell membrane causing leakage	Dental, textiles, paper, water treatment, wound dressing, surgical masks
Copper	Cheap	Tend to oxidize easily, less studied than Ag or Au NPs	Adhesion to cell wall, resulting in cavities/pits in the cell wall	Dental, wound dressings, water treatment
Gold	Effective, can be biosynthesized with bacteria	Expensive	Leakage of cellular contents, interaction with DNA	Textiles
Metal oxides	Antibacterial effectiveness	Toxicity (for some)	Production of ROS (reactive oxygen species)	Water treatment, wound dressings
Carbon (graphite and graphene)	Numerous morphologies	Toxicity	Leakage of cellular contents, extraction of phospholipids	Paper, dental

Table 1: An overview of materials with antibacterial effects [1-17].

Bacteria

Numerous types, gram-negative and gram-positive, and species of bacteria have been tested with nanomaterials. Common model bacteria such as *S. aureus* [18], *E. coli* [19], and *P. fluorescens* [20] have all undergone extensive testing with various nanomaterials. However, emphasis is mainly placed on nanomaterials with commonly known antibacterial effects, such as silver, copper, zinc oxide, and gold [21-23]. A potential area of research remains in both nanomaterials and applications that have been recently discovered or have been less scrutinized. One such application (microbial contamination in metalworking fluids) is discussed in the appendix.

Research on multiple types of bacteria is important due to their different structures, and hence different mechanism of resisting treatment. Figure 1 displays the morphological

difference between gram-positive (such as S. aureus) and gram-negative (such as *E. coli* and *P. fluorescens*) bacteria. Gram-negative bacteria are generally more resistant to treatment due to their thicker cell wall [24].

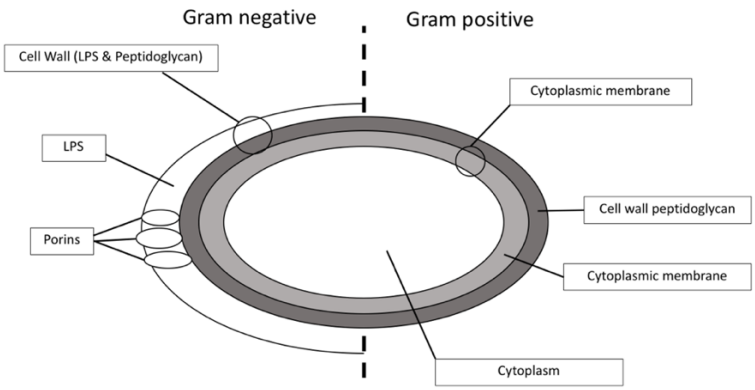

Figure 1: Differences in morphology between gram-negative and gram-positive bacteria

Bacterial growth refers to the increase in size of individual cells. Proliferation of bacteria refers to the increase in the number of cells through reproduction [25]. Bacteria treatment methods fall into two main categories based on their mechanisms of action – bacteriostatic and bactericidal [26]. Bacteriostatic treatments stop bacteria from reproducing and prevents the proliferation of the culture, while not necessarily killing the bacterial cells. Bactericidal treatments work by directly killing bacterial cells [27]. While at first glance bactericidal treatments may seem superior to bacteriostatic biocides, it needs to be remembered that the success and flourishment of bacteria depends on the cultures' ability to reproduce and proliferate. Due to the short life span of bacteria, bacteria cultures that cannot reproduce will die out quickly. Hence, depending on the mechanism and kinetics of the biocide, bacteriostatic treatments can be as effective as bactericidal treatments in dealing with the issue of microbial contamination [26].

Toxicity

Much remains unknown about the toxicity of nanomaterials. Despite the relatively long history of nanomaterial fabrication and application, little is known about the effects

on environmental health and safety [28]. NPs and "ultrafine" particulates have been linked to cardiovascular disease and respiratory illnesses in humans [29]. Nanomaterials can cause classical toxicology assays to have variable results, making the tracking and assessing of the effects of nanomaterials difficult [30].

Reusable nanomaterials treatments remain an area of great interest, both to reduce costs and avoid unintended environmental effects. This is particularly in areas of application such as water treatment, where the chance of environmental exposure is high. Dong et. al and Yao et. al both showed that N-Halamine nanoparticles have potential as a reusable antibacterial agent due to its magnetic properties [31, 32]. Tian et. al fabricated a magnetic graphene-based nanocomposite that displayed antibacterial effects against *S. aureus*. Similar to the N-Halamine nanomaterials, this magnetic property allows for the treatment to be reusable. Reusable nanomaterials also have the likelihood of reducing the cost of treatment. Material does not need to be constantly added and could reduce both cost and waste stemming from treatment.

Morphology and Mechanisms

The size and shape of nanomaterials greatly influences their properties. Solubility, surface area, agglomeration, and more are all highly dependent on nanomaterial morphology. Hunt et. al showed that smaller Ag nanoparticles had higher levels of toxicity and uptake compared to larger particles [33]. Sadeghi et. al demonstrated that both the shape and size of Ag nanoparticles was instrumental in their antibacterial effects against both *S. aureus* and *E. coli* [34]. This study showed that Ag nanoparticles with higher surface area (nanoplates) had a greater antibacterial effect compared to nanorods and nanoparticles, which both have smaller surface areas. This size effect for Ag NPs has been reported multiple times in literature [35, 36]. This effect is important for future research dealing with antibacterial nanomaterials. While Ag NPs have been closely studied, many other materials that show antibacterial effects have not been studied as closely, particularly with the same rigor in regard to morphology. Size and shape need to be considered in addition to chemical makeup in the fabrication and testing of future materials.

Antibacterial activity can vary with different bacteria. Kim et. al showed that antibacterial nanomaterials can have different effects for different bacteria [37], especially for silver nanoparticles. This shows that along with the morphology of the nanomaterial, the morphology of the bacteria cell is also of great importance. Other nanoparticles, such as zinc oxide, show antibacterial effects against multiple types of bacteria [13]. Materials that show wide ranging effects against multiple types of bacteria have potential to be bacterial treatments in industry, where wide ranges of bacteria species are observed (for example, over 100 species of bacteria have been observed in metalworking fluids, including gram-positive, gram-negative, and mycobacteria species [46, 49, 56, 57, 58]).

The morphology of antibacterial nanomaterials greatly influences its antibacterial effects. Hui et. al showed that the availability of the basal planes of graphene oxide is of great important to its antibacterial properties [38]. Liu et. al showed similar findings with graphene, and also emphasized the effects of lateral dimension and how it affected the mechanism of treatment [39]. Akhavan showed that the "sharp" shape of graphene and graphene oxide nanowalls contributed to their antibacterial effects [40]. Tu et. al used both TEM and molecular dynamics that the sharp morphology of graphene nanosheets (size of approximately 205nm lateral dimension and 1nm thick) can cut through the cell wall and extract phospholipids from *E. coli*, leading the cell death [41]. *E. coli* cells are approximately 0.5 um in width by 1 um in length. Three stages of this degradation process were observed under TEM – (1) initial toleration by *E. coli* of the nanosheets at low concentration, (2) damage to the cellular membranes, and (3) the cells losing their cellular integrity through membrane damage and cytoplasm loss. Two types of mechanisms were seen in the molecular dynamics simulation – an initial cutting and insertion of the nanosheets into the *E. coli* cellular membrane and extraction of the phospholipids from the membrane. The strong attraction between the graphene and phospholipids, due to the sp^2 configuration of the carbons in the graphene, led to this extraction. Simulations were performed for nanosheets with varying lateral sizes of 50 to 500nm (with that same thickness), all of which showed similar mechanisms. The antibacterial effect was greater

for greater lateral dimensions. This study gives evidence that a physical-based treatment with “sharp” nanomaterials has potential for treatment of bacteria.

Compared to nanomaterials that rely on cellular uptake, these more “physical” treatments of bacteria are of great interest due to the possibility of fabrication of surfaces with similar properties. Fabrication of durable surfaces that can be reused and possibly cause less environmental damage and toxicity compared to loose nanomaterials. Antibacterial surfaces utilizing nanoparticles and nanostructures is another hot area of research, particularly in orthopedics [42]. Silver NPs have been successful immobilized on surfaces with antibacterial effect [43, 44]. These surfaces were fabricated with multiple substrate materials and killed the bacteria on contact without the need for cellular uptake. Nanomaterial treatments with mechanisms that rely on contact with the exterior of the bacteria have the potential for reusable and more durable treatments in the form of nanostructures on surfaces. The nanostructure can remain attached to the surface while still interacting with and treating the bacteria.

Conclusion

Numerous nanomaterials have been shown to have antibacterial effects. A large range of morphologies, mechanisms, and materials have shown to be effective for different types of bacteria. The material and morphology combinations lead to the different mechanisms observed. Much study has been done on common nanomaterials, such as silver, copper, gold, and zinc oxide. While viability as antibacterial treatments of these many nanomaterials have been proven *in vivo*, much remains to be discovered on the toxicity and environmental effects of these materials. Due to the differences versus bulk materials, these nanomaterials can be difficult to control, and could possibly have unintended and far-reaching effects on the environment and in the human body. Previous study indicates the strong potential of new nanomaterials for antibacterial treatment, particularly those that are environmentally-friendly. Fabrication and testing of new nanomaterials, with an emphasis on morphology could lead to potential bacteriostatic or

bactericidal treatments. Research on more controllable and reusable nanomaterials is of great interest.

CHAPTER II

MOTIVATION AND OBJECTIVES

Numerous nanomaterials have been shown to have antibacterial properties. As discussed in Chapter 1, both the chemical makeup and the morphology of nanomaterials are important properties in effectively treating bacteria. Surfaces that have inherent antibacterial effects could be used for a wide range of applications including water treatment, medical implants, and reducing microbial contamination in industrial manufacturing. Current research on antibacterial surfaces generally focuses on chemically modifying the surface with materials such as silver, copper, and titanium dioxide that have known antibacterial effects. The morphological characteristics of these materials has been shown to play a significant role in the antibacterial properties. While much research has been carried out for the previously discussed materials, there remains a gap on the antibacterial properties of less common nanomaterials, especially for nanostructured surfaces. This research attempts to develop nanomaterials, particularly nanostructured surfaces, that can be used as passive treatments (i.e. where more treatment does not need to be continually added, such as with biocides) in order to producing effective and environmentally-friendly treatments against bacterial contamination.

2.1 Objectives

In order to prove the hypothesis, there are three main objectives for this research. The objectives are presented in a flow chart below in Figure 2.

Objective 1, identification of effective nanoparticles affecting bacteria

Objective 2, identification of nanostructured materials that have potential to treat bacteria

Objective 3, generating understanding of the material-bacteria interaction

To obtain the objectives, the following experimental tasks are proposed:

1) *Nanomaterial fabrication*

   The research will begin by fabricating various nanoparticles and nanostructures for testing with bacteria. The research starts with fabricating nanoparticles that have been studied in literature [1-2,7,121-122]. Nanostructures on metallic substrates will then be fabricated, with focus of substrate surface preparation and nanostructure coating generation. Specific emphasis will be placed on the morphology of the nanomaterials. Fabrication will take place concurrently with the bacteria testing in objectives (2) and (3) so that the fabrication methods and focus can be adjusted as results are found. Materials are analyzed using surface roughness, optical microscopy, and SEM.

2) *Nanoparticle bacteria testing*

   Nanoparticles will be cultured with bacteria cells *in vitro* to observe antibacterial effects. Based on these results, a nanostructure using similar chemical and morphological makeup will be fabricated and testing in (3). Bacteria concentration is testing with luminescence and by

3) *Nanostructure bacteria testing*

   A new testing protocol will be developed to test antibacterial coatings against a control substrate with a coating. The nanostructures fabricated in (1) will be tested here. A key factor that also needs to be considered is the durability of the coating. Coatings that lack durability and leach into the liquid during testing limit reusability and may not be suitable for future application. Further testing is done to ensure the consistency and validity of the testing process. Luminescence and SEM are used to analyze the reduction in bacteria load and changes to bacteria morphology, respectively.

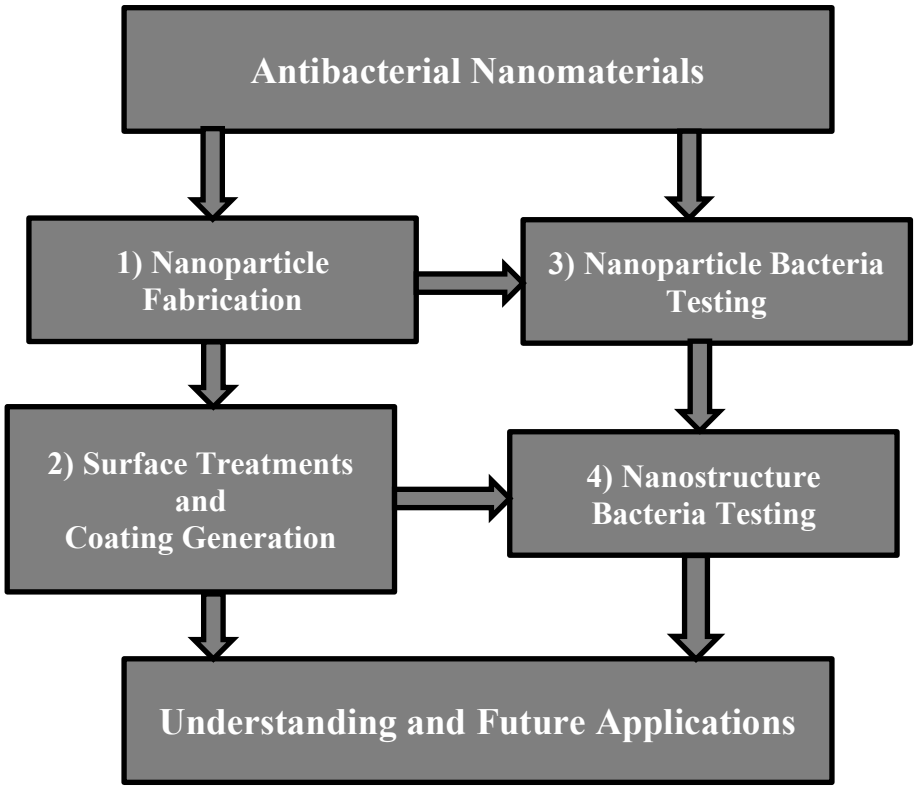

Figure 2: Research flow chart

2.2 Thesis Structure

Chapter 1 provides background information about antibacterial nanomaterials, with emphasis on nanomaterial morphology and physical mechanisms. A potential application for the research in this thesis is also discussed in detail – microbial contamination of metalworking fluids. Motivations and objectives for the research are presented in Chapter 2.

Chapters 3 and 4 consist of nanomaterial fabrication – nanoparticles in Chapter 3 and surface treatment and nanostructure coating generation in Chapter 4. The fabrication of V_2O_5 nanomaterials is discussed in Chapters 3 and 4. Vanadium pentoxide nanomaterials have been shown to be useful additives in batteries due to their excellent electrical and thermal properties [45-47]. Multiple morphologies have been fabricated in literature, including nanowires [48], rods [49], spheres [50], sheets [51], and tubes [52].

The resulting morphologies rely heavily on the methods of fabrication [53]. Few studies the antibacterial performance of V_2O_5 nanomaterials, with research contained to nanowires [48] and silver-loaded V_2O_5 nanotubes [54].

Bacteria testing with nanoparticles in discussed in Chapter 5, while bacteria testing with nanostructures on metallic substrates is presented and discussed in Chapter 6. Chapters 5 and 6 of this research tests the treatment of bacterium *Staphylococcus aureus* with various nanomaterials *in vitro*. *S. aureus* is a gram-positive, spherical bacterium (cocci) that is commonly found on human skin, nose, respiratory tract, and the lower reproductive tract in women. *S. aureus* can form "grape-like" clusters and causes a wide variety of diseases. The organism is a chemoorganotrophic (can oxidize chemical bonds in organic compounds for energy) and is a facultative anaerobe (can grow without oxygen) [55].

20-30% of humans carry *S. aureus* on their bodies [56]. The bacteria are not always pathogenic (only certain strains are virulent). These virulent strains can cause a variety of infections, ranging from common to life-threatening. One of five most common causes of hospital-acquired infections [57]. Approximately 50,000 deaths each year are caused by *S. aureus* [58]. Wound infections after surgery and biofilms on medical devices in human body or on human tissue are one of the most common causes of infection.

S. aureus has high levels of antibiotic resistance, particularly β-lactam antibiotics due to its production of β-lactamase [59]. Methicillin-resistant *Staphylococcus aureus* (MRSA) is of particular concern and can cause dangerous infections. New methods of treatment of *S. aureus* are an important area of research and are investigated further on.

Conclusions and future research are discussed in depth in Chapter 7.

CHAPTER III

NANOPARTICLE FABRICATION

Three different types of nanoparticles were fabricated for this experiment – Zirconium phosphate (ZrP), Yttrium oxide (Y_2O_3), and Vanadium oxide (V_2O_5). All three used a hydrothermal method for preparation. Different morphologies resulted for each nanoparticle – nanoplatelets for the ZrP sample, a mixture of nanotubes and nanosheets for the Y_2O_3 sample, and nanosheets for the V_2O_5 sample. All chemicals in these studies were purchased from Sigma-Aldrich.

3.1 ZrP Nanoplatelets

The method used to fabricate the ZrP nanoplatelets was derived from literature [45, 60]. ZrP nanoplatelets can be prepared with a variety of methods including a reflux method, hydrothermal method, and hydrofluoric acid method. Zirconium phosphate nanoparticles were prepared with a hydrothermal method. The hydrothermal method allows for higher aspect ratios for the nanoplatelets in comparison to the reflux method, as well as more consistent sizes for the nanoplatelets [60]. This method also is safer than the hydrofluoric method due to the lack of HF in the process. These nanoplatelets have been shown in literature to have anti-wear and lubricating properties.

ZrP Nanoplatelet Synthesis

1) 4.0g of zirconyl chloride octahydrate ($ZrOCl_2 \cdot 8H_2O$, >99.0 wt%, Sigma-Aldrich) was mixed with 40.0 mL of 12M H_3PO_4.
2) The solution was transferred to a Teflon-lined pressure vessel. The vessel was sealed and heated to 200°C for 24 hours.
3) The products were washed with DI water and centrifuged at 5000rpm three times.
4) Dried at 65°C for 24 hours.

5) The resulting product was collected and ground with a mortar and pestle into a powder.

Analysis

Previous studies have characterized these nanoplatelets with optical microscopy, SEM, AFM, and XPS to verify morphology and chemical composition. The resulting morphology was α-ZrP nanoplatelets of approximately 1μm in lateral dimension with a thickness 200-400 times thinner than the lateral dimension [45, 60].

3.2 V_2O_5 Nanoparticles

Vanadium oxide (V_2O_5) nanoparticles were fabricated with a hydrothermal process as used previously in literature [46, 61, 62]. The nanoparticles were made in conjunction with a V_2O_5-based nanostructure, which is discussion in detail in Chapter 4. First, a V_2O_5 precursor was prepared in a reaction with H_2O_2. The precursor underwent a hydrothermal process to obtain a final product of V_2O_5 nanoparticles.

V_2O_5 precursor preparation

1) Suspend 0.5 mmol (90.9 mg) of V_2O_5 bulk powder (99.99%) in 23.5 mL of DI water with magnetic stirring
2) When fully combined (uniform appearance), 1.5 mL H_2O_2 solution (30% w/w in H2O) was added dropwise (while still stirring)
3) Bubbles formed as the H_2O_2 solution was added and stirred
4) The suspension became clearer and more transparent after approximately 40 minutes of stirring

Precursor reaction after mixing V_2O_5 powder and H_2O_2 solution:

$$V_2O_5 + 4H_2O_2 \rightarrow 2[VO(O_2)_2(OH_2)]^- + 2H^+ + H_2O$$

$$V_2O_5 + 2H^+ + 4H_2O_2 + 3H_2O \rightarrow 2[VO(O_2)(OH_2)_3]^+ + O_2$$

$$2[VO(O_2)_2(OH_2)]^- + 4H^+ + 2H_2O \rightarrow 2[VO(O_2)(OH_2)_3]^+ + O_2$$

$$2[VO(O_2)(OH_2)_3]^+ \rightarrow 2[VO_2]^+ + O_2 + 6H_2O$$

Synthesis of V_2O_5 nanoparticles

1) V_2O_5 precursor suspension was added to a Teflon hydrothermal autoclave
2) Ni/Porous Ni substrate (as described in Chapter 4) was added directly into the suspension
3) Autoclave was sealed and underwent the autoclave process for 7 hours at 180°C
4) Autoclave cooled naturally in the air
5) Autoclave chamber was opened, and three products were found: black Ni/Porous Ni/V_2O_5 samples, a green precipitation, and clear colorless liquid
6) The precipitant and the black Ni/Porous Ni/V_2O_5 samples were cleaned with ethanol and DI water, dried in vacuum chamber overnight at 70°C
7) Annealed for 30 minutes at 350°C
8) The resulting product is a dark brown powder of V_2O_5 nanoparticles.

Analysis

The resulting morphology of the nanoparticles made with this method are nanosheets, as seen in literature [51]. Dimensions of the nanosheets range from 500nm to tens of microns. Morphology of these nanosheets grown directly on a substrate (as seen in Chapter 4) hints that the lateral dimensions of the nanosheets may be from 2-5μm, but this needs to be affirmed through further testing. Additional analysis, particularly with SEM and EDS, should be performed in order to validate both the chemical composition and morphology of the fabricated nanomaterials.

3.3 Y_2O_3 Nanotubes and Nanosheets

The method used for fabrication is found in literature [63]. Erbium-ytterbium-doped yttrium oxide nanoparticles (Y_2O_3:Er^{3+}, Yb^{3+}) were prepared with a hydrothermal method. The resulting morphology was a mix of nanotubes and nanosheets. Different morphologies can be fabricated by changing the reaction temperature and pH values. These nanoparticles have been shown in literature to have applications in bioimaging [64], optical engineering [65], and lubrication [66, 67].

Preparation of Y_2O_3 nanotubes and nanosheets

1) 1.34g of Y_2O_3 powder (>99.99%, Sigma-Aldrich) was dissolved into 250 mL of HNO_3 solution (2.8 wt%) at 60°C. This produced a transparent yttrium nitrate solution.
2) 27 mg of $Er(NO_3)_3 \cdot 5H_2O$ and 3 mg of $Yb(NO_3)_3 \cdot 5H_2O$ was added to the solution
3) The pH of the solution was adjusted to 7.0 by adding a KOH solution (15 wt%)
4) After adding the correct amount of KOH solution, the resulting volume was 900 mL
5) This solution was transferred into a 2L Teflon-lined pressure vessel. The vessel was sealed and heated to 200°C for 12 hours
6) The vessel was let to naturally cool to room temperature.
7) The precipitation was collected with centrifugation, washed with DI water three times, and dried at room temperature. This yielded a resulting precursor.
8) The precursor was then calcined at 1000°C for 3 hours in air to yield a mixture of Y_2O_3:Er^{3+}, Yb^{3+} nanotubes and nanosheets.

Analysis

TEM imaging was used in literature to analyze the fabricated nanotubes and nanosheets. The nanotubes were 200nm long, with diameters ranging from 20-50nm. The

nanosheets were approximately 250nm in lateral dimension. A high amount of crystallinity was observed in the samples. XRD was also used to confirm the chemical composition of the samples.

CHAPTER IV

FABRICATION OF NANOSTRUCTURED MATERIALS

The goal of the surface treatment and coating generation was to fabricate nanostructured material containing V_2O_5 nanoparticles on a metallic substrate. The two main methods were a hydrothermal method and spin-coating. Multiple base substrate materials were used – namely nickel, aluminum, copper, and steel. These substrates are widely found and are common in many industrial applications. Surface preparation methods included sanding, chemical etching, electrodeposition, and leaving the surface as-received. SEM, optical microscopy, and roughness testing were used to analyze the samples, both for the surface preparation and the coating generation.

4.1 Surface Preparation

Materials

Materials were selected upon ease of availability and to have a diversity of different substrate materials. Aluminum, steel, copper and nickel were selected as possible substrates for the coating generation. The nickel selected (alloy 200/201, shim stock, 0.13mm thickness) had already been successfully fabricated with a V_2O_5 nanostructure in literature [47]. Images of the bulk material and substrate composition are below.

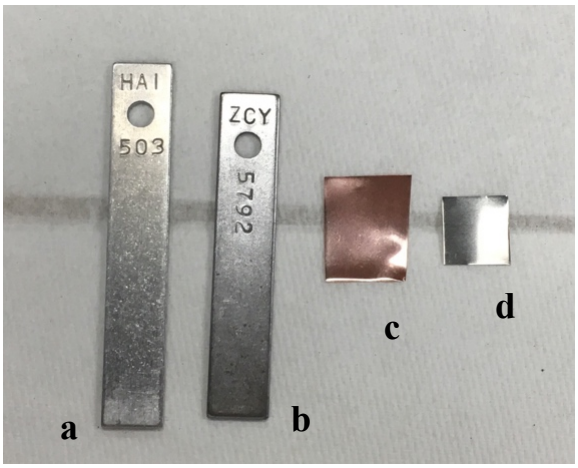

Figure 3: Bulk images of 4 selected substrate materials (from left) (a) aluminum corrosion coupon, (b) steel corrosion coupon, (c) copper shim stock, and (d) nickel shim stock

Substrate materials composition, heat treatment, and grain structure

Aluminum corrosion coupon, T6 heat treatment

Composition		Si	Fe	Cu	Mn	Mg	Cr	Zn	Ti
6061 alloy	Max	0.8	0.7	0.40	0.15	1.2	0.35	0.25	0.15
	Min	0.40		0.15		0.8	0.04		

Steel corrosion coupon, 883673 heat treatment

Composition	C	Mn	P	S	Si	Ni	Cr	Mo	Al	Cu
1010 alloy	0.090	0.380	0.009	0.010	0.012	0.030	0.046	0.010	0.039	0.038

Nickel Shim Stock

Composition		Ni	Fe	C	Mn	Si	Cu	S
Ni 200/201	Max		0.40	0.15	0.35	0.35	0.25	0.01
	Min	99.0						

Copper shim stock

Composition		Cu	O
110 Cu	Max	99.9	
	Min		0.05

Of the substrates used for fabrication, aluminum, copper, and nickel have a face-centered-cubic (FCC) structure. In contrast, at room temperature, the steel sample used has a body-centered-cubic (BCC) structure.

Methods

Multiple methods of surface treatment were attempted before coating generation. The aim of the study was to find a low cost and efficient method of surface treatment that yielded a suitable coating. The four methods of surface treatment included sanding, chemical etching, electrodeposition, and as-received (no surface treatment). Materials were prepared in conjunction with the bacteria experiments in Chapter 6, so certain materials were eliminated due to other factors. This is described in detail in Chapter 6. The table below gives a summary of the surface treatments attempted.

	Material			
Surface Treatment	Aluminum	Copper	Nickel	Steel
As-received	x	x	x	x
Sanding	x	x	x	x
Chemical etching			x	
Electrodeposition			x	

Table 2: Surface preparation methods of metal substrates

As-received: Materials were ultrasonically cleaned in acetone, DI water, and ethanol.

Sanding: Materials were wet sanded with 400 grit silicon carbide sandpaper and water. The materials were then cleaned with acetone, DI water, and ethanol.

Chemical etching: Nickel was etched with 3M HNO_3. The substrate was then cleaned with DI water, acetone, and ethanol.

Electrodeposition: Nickel was prepared with an electrodeposition process using a salt and an anode. Two materials were used for as anodes: a carbon rod and another piece of cleaned nickel. The resulting structure was a Ni/Porous Ni substrate.

Ni/Porous Ni substrate preparation with electrodeposition

1) Cleaned with DI water, 0.1M HNO_3, and ethanol (90%) and dried
2) Electrodeposition
    a. Cathode: Ni sheet (99.0% Ni, 0.13mm thick)
    b. Anode
        i. Graphite rod (99.995% carbon, 6mm thick)
        ii. Ni sheet (same as cathode)

        Note: two different anodes were used and compared (separately, not at the same time)
    c. Aqueous electrolyte of 0.2M $NiCl_2$ (98%) and 4.0M NH_4Cl (>= 99.5%)
    d. Current density of 0.5 A/cm^2 for 7 minutes
3) Rinse with acetone, DI water, and ethanol
4) Vacuum dried overnight at 70°C

The electrodeposition process attempts to fabricate a porous surface on the nickel substrate. This porous structure consisted of micro-channels of 10-20μm in diameter as described in literature [47]. The resulted from the streams of H2 bubbles during the electrodeposition process. Initially, the carbon rod was used as an anode. The anode was switched to a Ni sheet after difficulty in producing a consistent surface (to the naked eye) during the process. Images of the electrodeposited surfaces can be seen in Figure 9 and in literature [47].

Sample Analysis

Surface Roughness

Surface roughness was characterized with a Mahr Perthometer M2. This instrument uses a stylus tip in contact with the surface to measure surface roughness. Three measurements were taken for each material and surface treatment combination (in different locations on the surface) and averaged. This allowed for a consistent and accurate characterization of the surface roughness for each sample. Ra is the average roughness, the arithmetic average of the surface profile, and Rz is the mean roughness depth (with five sampling lengths of 0.8mm). Surface roughness is taken over each sampling length and then averaged.

Figure 4: Mahr Perthometer M2 used for surface roughness measurements

Surface Treatment	Method	Material (results in μm)							
		Aluminum		Copper		Nickel		Steel	
		Avg	Std Dev	Avg	Std Dev	Avg	Std Dev	Avg	Std Dev
As-received	Ra	0.205	0.030	0.264	0.006	0.286	0.015	0.828	0.036
	Rz	1.86	0.33	1.74	0.11	2.18	0.07	4.76	0.36
Sanding	Ra	0.234	0.035			0.292	0.005	0.589	0.052
	Rz	2.03	0.03			2.63	0.11	3.22	0.19
Chemical etching	Ra					0.138	0.012		
	Rz					1.14	0.10		
Electro-deposition	Ra					7.537	0.915		
	Rz					39.70	3.65		

Table 3: Surface Roughness of metal substrates after surface preparation (results in μm). The sampling length used was 0.8mm. Note the high surface roughness for the electrodeposited surface. Standard deviations for all materials are within acceptable ranges in comparison to the means for both Ra and Rz measurements.

Microscopy

Prepared substrates were analyzed with a Keyence VHX-600K Digital Microscope. Samples were cleaned with DI water, acetone, and ethanol before microscopy to minimize contamination. Surface roughness and morphology were compared for each sample under a magnification of 200x. The electrodeposited surfaces of nickel were further analyzed with SEM, allowing a greater level of detail into the morphology. The analysis of the surface finishes before attempting coating generation may hint as to why certain combination of material and surface finish were successful while others were not.

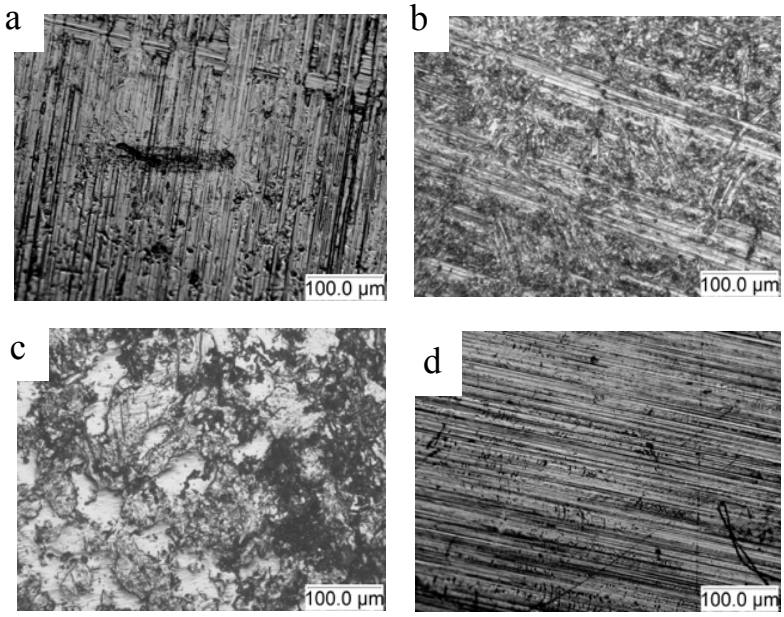

Figure 5: As-received/cleaned (a) nickel, (b) aluminum, (c) steel, (d) copper as viewed under an optical microscope (200x)

The as-received and cleaned samples had a wide range of surface finishes. This was expected as the nickel and copper samples were very smooth in comparison to the corrosion coupon samples of aluminum and steel.

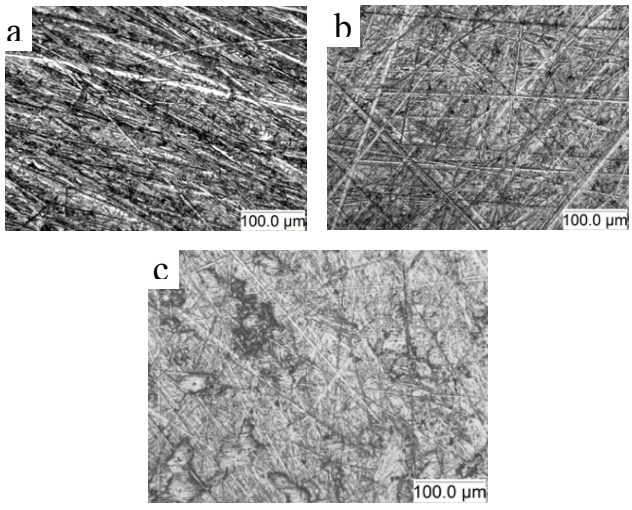

Figure 6: Sanded (400 grit, silicon carbide paper) (a) nickel, (b) aluminum, (c) steel

Sanding the samples resulted in more uniform surfaces that were similar in comparison to the other materials. This allowed the effects of the material irrespective of surface finish to be compared in the coating generation process further on.

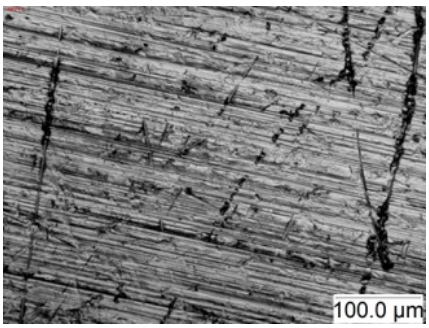

Figure 7: Nickel etched with 3M nitric acid (HNO3) imaged with an optical microscope (200x)

The nickel etched surface did not yield a visible change in comparison to the as-received nickel in the Figure 5.

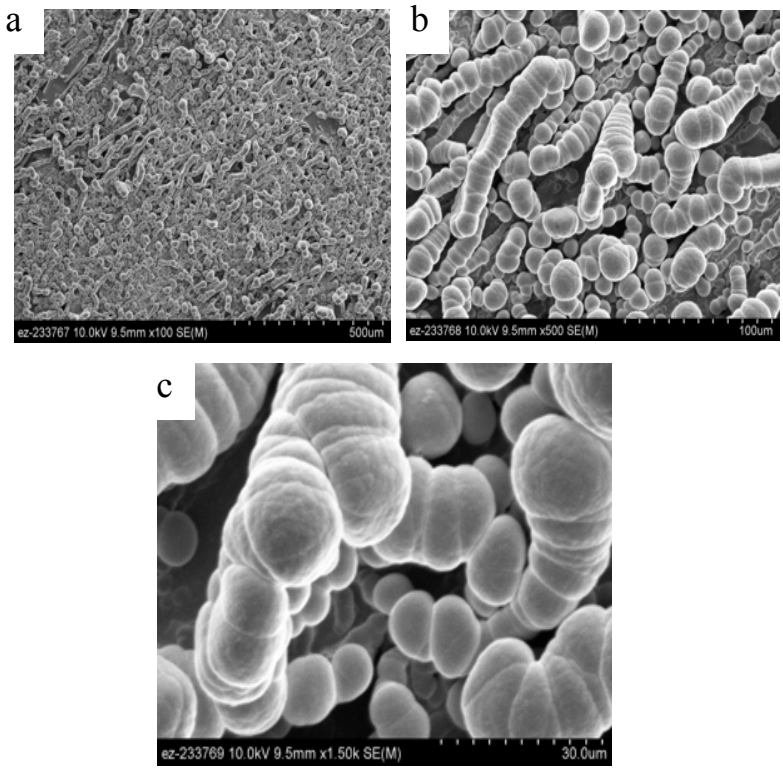

Figure 8: Nickel with electrodeposition (nickel as anode) viewed with SEM (a) 100x, (b) 500x, (c) 1500x

The resulting morphologies of the electrodeposited nickel were quite different (Figure 8 for the nickel sheet anode and literature for the carbon rod anode [47]). This in turn led to the nickel-V_2O_5 nanocomposite using the carbon anode electrodeposition having a more uniform distribution of V_2O_5 flowers compared to the nickel anode electrodeposition sample. The porous morphology of the nickel electrodeposited with the carbon rod has a more uniform morphology that may lead to better growth and deposition of the V_2O_5 nanostructure. In addition, the surface roughness values of the electrodeposited surfaces were much higher than the other surface preparation methods. This morphology difference is important and may play a role in the mechanism of treatment discussed in Chapter 6.

4.2 Coating Generation

Two different methods were used to generate a V_2O_5 coating on the metallic substrate – spin-coating and a hydrothermal method. Successful coating was achieved with the nickel substrates treated with electrodeposition followed by a hydrothermal process. Other methods, substrates, and pre-coating generation surface treatments did not achieve the same level of consistency – both when viewed in bulk and under microscopy (optical and SEM).

Hydrothermal Method

V_2O_5 Nanostructure on Nickel/Porous Nickel Substrate

The methods used below are described in literature [111]. A V_2O_5 precursor was first made, followed by a hydrothermal method, vacuuming drying, and annealing. The formation of V_2O_5 nanosheets on the electrodeposited nickel surface resulted from 2-dimensional growth during the hydrothermal process. The porosity of the FCC-structured nickel allowed for the growth of the nanosheets directly on the substrate. The annealing process further increased the crystallinity. This growth mechanism was proposed and validated with SEM at various timepoints in literature [47]

V_2O_5 precursor preparation

5) Suspend 0.5 mmol (90.9 mg) of V_2O_5 bulk powder (99.99%) in 23.5 mL of DI water with magnetic stirring
6) When fully combined (uniform appearance), 1.5 mL H_2O_2 solution (30% w/w in H2O) was added dropwise (while still stirring)
7) Bubbles formed as the H_2O_2 solution was added and stirred
8) The suspension became clearer and more transparent after approximately 40 minutes of stirring

Precursor reaction after mixing V_2O_5 powder and H_2O_2 solution:

$$V_2O_5 + 4H_2O_2 \rightarrow 2[VO(O_2)_2(OH_2)]^- + 2H^+ + H_2O$$

$$V_2O_5 + 2H^+ + 4H_2O_2 + 3H_2O \rightarrow 2[VO(O_2)(OH_2)_3]^+ + O_2$$

$$2[VO(O_2)_2(OH_2)]^- + 4H^+ + 2H_2O \rightarrow 2[VO(O_2)(OH_2)_3]^+ + O_2$$

$$2[VO(O_2)(OH_2)_3]^+ \rightarrow 2[VO_2]^+ + O_2 + 6H_2O$$

Synthesis of V_2O_5 nanosheet structure

9) V_2O_5 precursor suspension was added to a Teflon hydrothermal autoclave
10) Ni/Porous Ni substrate was added directly into the suspension
11) Autoclave was sealed and underwent the autoclave process for 7 hours at 180°C
12) Autoclave cooled naturally in the air
13) Autoclave chamber was opened, and three products were found: black Ni/Porous Ni/V_2O_5 samples, a green precipitation, and clear colorless liquid
14) The precipitant and the black Ni/Porous Ni/V_2O_5 samples were clean with ethanol and DI water, dried in vacuum chamber overnight at 70°C
15) Annealed for 30 minutes at 350°C

Analysis

The as-fabricated Ni/V_2O_5 nanocomposite was analyzed with SEM. XRD has also been used for analysis in literature [47]. Figure 9 shows the morphology of the sample with electrodeposition with nickel. The morphology of the carbon anode electrodeposition can be seen in literature [47]. The Ni/V_2O_5 nanocomposite resulting from the nickel sheet electrodeposition was imaged with a Hitachi S4800 SEM. The samples in literature are

more clearly defined and higher consistency than that in Figure 9. The differing electrodeposition materials is on clear importance.

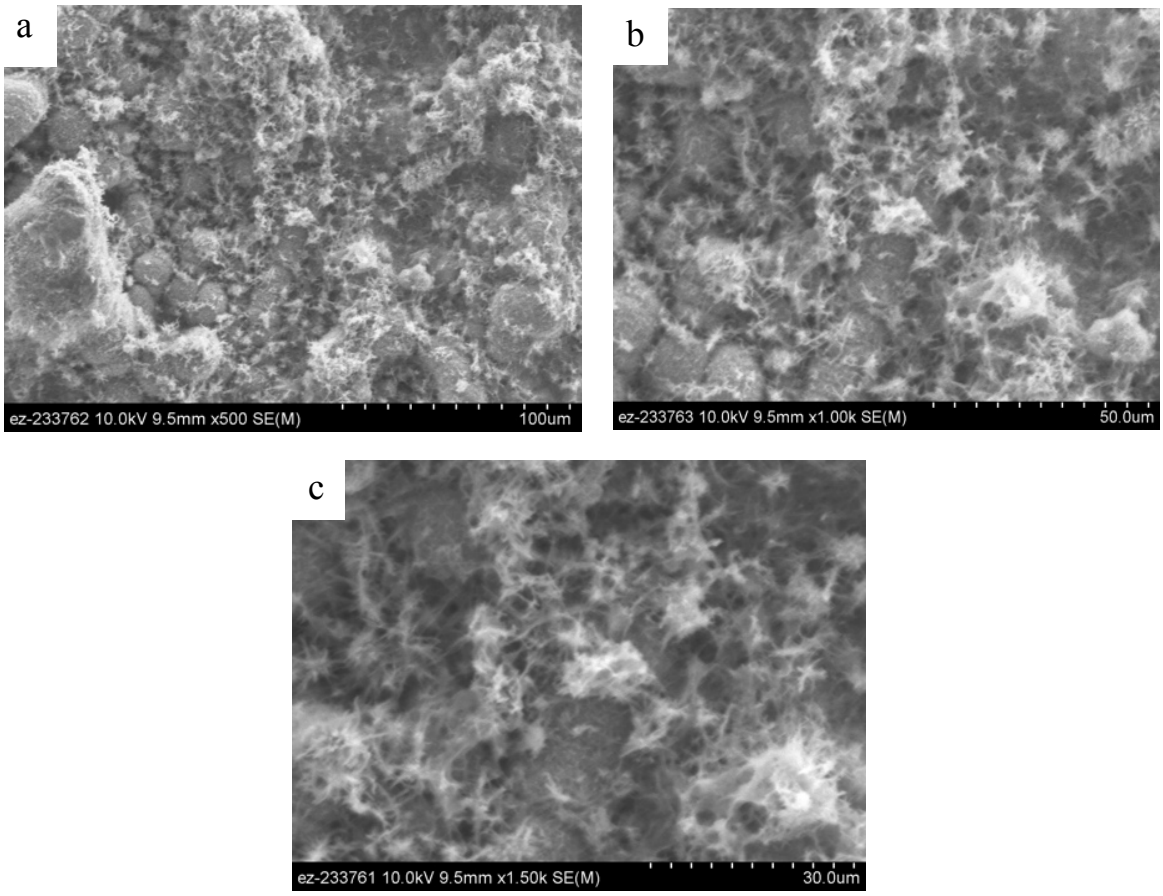

Figure 9: V_2O_5 nanostructure on nickel electrodeposited substrate (nickel as anode) viewed with SEM (a) 100x, (b) 500x, (c) 1500x

Other Substrate Materials

An identical hydrothermal method was done on copper, aluminum, steel, and nickel (with different surface preparations) substrates. The sanded copper substrate had a consistent black coating, similar to appearance to the nickel substrate. However, the coating came off of the substrate into liquid LB in the bacteria experiment (discussed in

Chapter 6), so the coating was unsuccessful. The as-received copper sample had a less consistent coating and also came off into the liquid LB (Chapter 6).

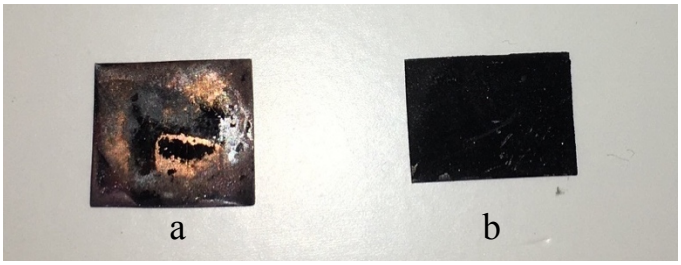

Figure 10: Unsuccessful copper coating generation (a) as-received and (b) sanded.

The aluminum substrates (as seen below) did not achieve consistent coatings. The coating was blotchy and varied from yellow to green to black in appearance.

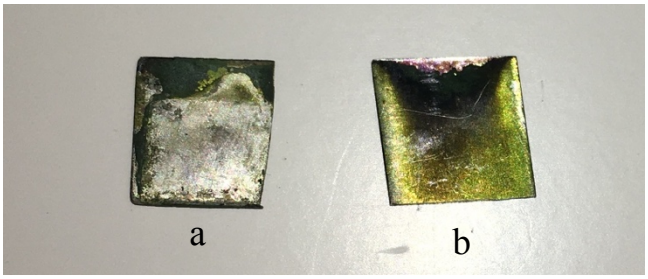

Figure 11: Unsuccessful aluminum coating generation (a) as-received and (b) sanded.

The coating did not adhere to the steel substrate at all (for both as-received and sanded sample), so that coating process was also unsuccessful. This was not surprising

due to the different crystal structure of the steel (BCC) compared to the electrodeposited nickel (FCC).

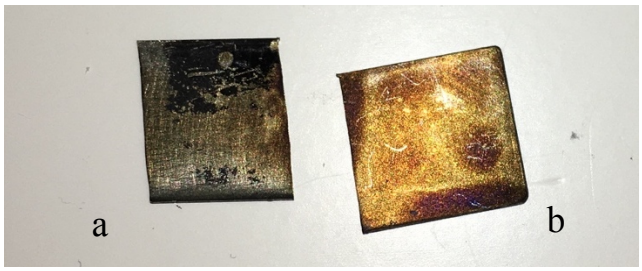

Figure 12: Unsuccessful steel coating generation (a) as-received and (b) sanded.

The nickel substrates without the electrodeposition also did not achieve consistent coatings. This shows that the electrodeposition process is an essential part of the Ni/V_2O_5 nanocomposite. The lack of porosity and growth sites for the 2-dimensional V_2O_5 nanosheets may have played a role in the unsuccessful deposition. The unsuccessful samples can be seen below.

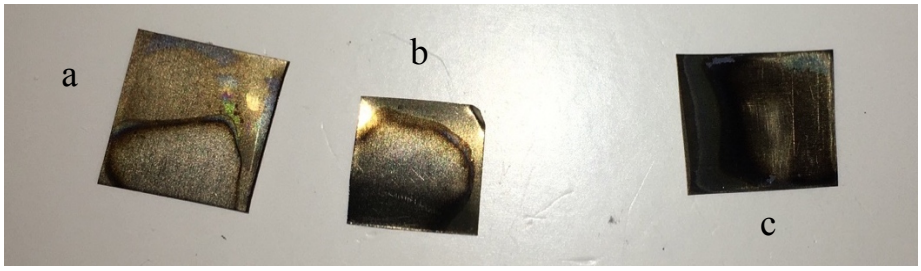

Figure 13: Unsuccessful nickel coating generation (a) as-received, (b) sanded, (c) chemically etched with HNO_3.

4.3 Discussion

Implications

These methods resulted in the successful fabrication of a 2-dimensional nickel-V_2O_5 nanocomposite. These materials went on to be tested with bacteria (Chapter 6). This research also attempted to find alternative methods of fabrication of the nanocomposite,

both in terms of different base materials, different surface treatments, and different coating generation methods. This morphology difference of the electrodeposited nickel surfaces is of particular importance and may play a role in the mechanism of treatment discussed in Chapter 6. The morphology and crystal structure of the electrodeposited nickel facilitated the growth of the 2D V_2O_5 nanosheets directly on the substrate and allowed for a consistent and nanostructured surface finish.

Limitations and Problems

Many of the coating generation attempts were unsuccessful. This came from various reasons, including inadequate attachment of the coating to the substrate (such as the hydrothermal method with the copper sample), inconsistency from sample to sample (such as the aluminum samples that underwent the hydrothermal method, as well as the nickel samples that did not undergo electrodeposition), and simply lack of any attachment whatsoever, as seen in the steel substrate.

There was also inconsistency in the electrodeposition of the nickel, as seen below. Variables, including time, voltage, surface area submerged, had to be carefully controlled to achieve a consistent surface treatment. A consistent surface was generally more easily

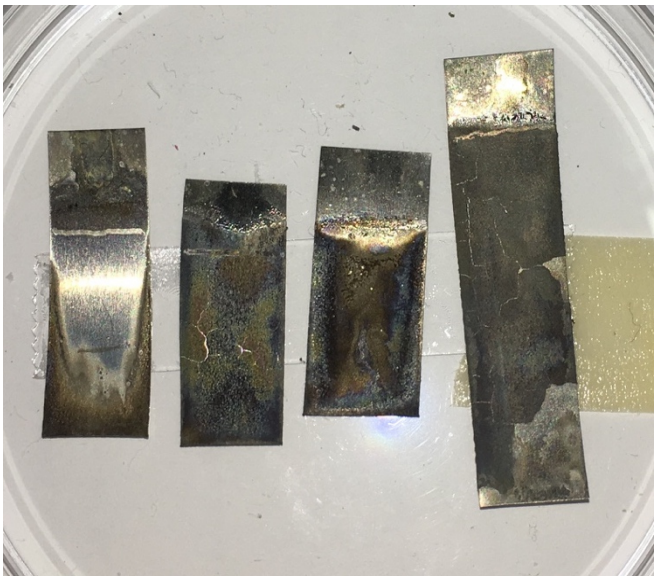

Figure 14: Poor electrodeposition on nickel substrate. Notice the inconsistency, corrosion, and flaking on the samples.

achieved with using nickel as the anode (in comparison with the carbon rod), however, this resulted in a different surface morphology for the nickel/porous nickel substrate, which then resulted in a different morphology for the nickel V_2O_5 nanocomposite. Hence, despite it being easier to electrodeposit with the nickel anode, it may be necessary to use the carbon anode if that specific morphology is desired.

Future Work

Scalability of the surface preparation and coating generations is important, specifically when certain applications are considered. Larger industrial applications (such as in a tank containing metalworking fluids) require much larger surface areas than other applications. Electrodeposition and the hydrothermal method used for the successful V_2O_5 coating generation are not as scalable as the other methods attempted. Future work can look at scaling up the scaling up the methods used, as well as attempted new methods that can achieve similar morphological and chemical properties. Certain combinations worked better than others, and many lessons were learned in the process.

Different surface treatments could also be attempted, particularly in sanded with a much coarser grit. The surface roughness of the electrodeposited nickel was much higher than the other surface treatments, so perhaps a different surface treatment that could produce similar roughness levels could be successful. Electrodeposition of nickel onto other substrates could also be attempted.

Further analysis of the samples, particularly with high-powered SEM and EDS, could help compare the different samples and potentially solve some of the issues in the fabrication process for the as-received, sanded, and etched samples. Copper has a natural antibacterial effect, so if a more stable coating could be achieved on the copper than perhaps this combination would be a better treatment than the nickel-V_2O_5 nanocomposite material. Further microscopy would allow the nanomorphology of other materials, like the copper-V_2O_5 nanocomposite to be studied in greater detail, and the methods and materials could possibly be improved.

CHAPTER V

EFFECTS OF NANOPARTICLES ON BACTERIA

This chapter discusses the treatment of methicillin-resistant *S. aureus* with various nanoparticles. Experiments were performed *in vitro* at the Texas A&M Health Science Center. Major results showed significant bacteria reduction with V2O5 nanoparticles, with a 92.4% reduction after 24 hours at a concentration 500μg/mL, and reductions of 96.7% and 94.3% with a concentration of 1mg/mL after 2 and 24 hours, respectively. Results were quantified in CFU/mL and used to show the potential of treatment of *S. aureus* with V_2O_5 nanoparticles. These experiments were performed as a baseline before the bacteria-nanostructured substrate tests described in Chapter 6.

5.1 Nanoparticles

The nanoparticles tested were V_2O_5, Y_2O_3, and ZrP. The NPs were fabricated with the methods described in Chapter 3. The V_2O_2 nanoparticles have a nanosheet morphology, as reported in literature [47, 62]. Y_2O_3 nanoparticles consisted of a mix of nanosheets and nanotubes, while the ZrP nanoparticles consisted of nanosheets with lateral dimensions of 1μm. Neither Y_2O_3 nor ZrP nanomaterials have been shown in literature to have an antibacterial effect. One study showed antibacterial activity for V_2O_2 nanoparticles, but for a different morphology (nanorods) [4], or in combination with Ag NPs, which have well known antibacterial effects [10].

The first step was to show that nanoparticles with specific morphologies are effective against bacteria. The V_2O_5 nanoparticles tested proved to be effective, as shown later on in this research. The next step for this research is further analysis with TEM to predict the antibacterial mechanism. This imaging may give insight into whether the treatment is bacteriostatic or bactericidal. At the beginning of this experiment, the initial concentration tested was 100μg/mL. This concentration, however, did not show a decrease in bacteria proliferation in any of the experimental samples compared to the control. The

concentrations were increased to 500μg/mL and 1 mg/mL, at which point decreases in bacteria proliferation were seen. The difference at 2 hours and 500μg/mL was not statistically significant, which may indicate that the MIC (minimum inhibitory concentration) for the treatment is between these two concentrations. Further treatment may allow for a MIC to be determined. More testing and analysis are needed before a conclusion can be formed.

5.2 Cell culture

S. aureus Xen36 was selected as the bacteria for this experiment. *S. aureus* is a common gram-positive bacterium used for *in vitro* study. The Xen36 strain contains a copy of the *Photorhabdus luminescens* lux operon, which gives the bacteria bioluminescence. This allows for real-time monitoring of the bacterial load during luminescence assays. Bacteria was cultured in liquid media in 96 well plates, and the initial and final bacteria concentrations were quantified in CFU/mL.

1) *S. aureus* Xen36 was inoculated into liquid LB and incubated overnight. The concentration was determined with a Nanodrop spectrophotometer and diluted to a starting concentration of $4.50*10^5$ CFU/mL with liquid LB.
2) 10mg of each nanomaterial was weighed.
3) An initial dilution of 10mg/mL for each nanomaterial sample was made with DI water and vortexed.
4) The samples were then diluted down to the desired testing concentrations of 500μg/mL and 1mg/mL with liquid LB containing *S. aureus*.
5) Using a 96 well plate, 150μL was deposited per well. The test was performed in triplicate (three wells were used per concentration).
6) Samples were incubated for both two and 24 hours at 37°C.
7) When the incubation period was finished, the samples were removed from the incubator and were testing for luminescence. Results were quantified in CPS

(counts per second). Three measurements were taken for each well and the results were recorded.

8) Based on the luminescence results, the CFU/mL was tested using serial dilutions and plate counting. 100 μL was deposited for three different concentrations (ranging from neat to 10^9) onto LB agar plates. Three depositions were performed for each concentration for each sample. These plates were incubated overnight before counting the plates. The CFU/mL for each sample was determined and recorded.
9) Samples for each liquid culture were fixed for further analysis. SEM and optical microscopy were used to analyze the resulting bacteria cell morphology and thereby predict the treatment morphology.

5.3 Effects of NPs on cells

Summary

The V_2O_2 nanosheets proved to be effective against *S. aureus*. Neither the ZrP nanosheets or the mixture of Y_2O_3 nanotubes or nanosheets were effective at either concentration or after either treatment time period.

Zirconium phosphate

The ZrP nanoparticles did not show an effect against *S. aureus*. The bacteria load was actually higher for the ZrP culture than the control for both NP concentrations and incubation times. The bacteria count ranged from 10% (1mg/mL, 2 hours incubation) to 61.3% (1mg/mL, 24 hours incubation) higher than the control, but neither of these differences is of statistical significance.

Vanadium oxide

Significant antibacterial activity was seen in the V_2O_5 sample at a concentration of 1mg/mL after 2 hours incubation (96.73% decrease) and at both 500μg/mL and 1mg/mL concentrations after 24 hours (92.44% and 94.30% decreases, respectively).

Yttrium oxide

The Y_2O_3 nanomaterials were also not effective against *S. aureus*. At the 500µg/mL concentration, after both 2- and 24-hours of treatment.

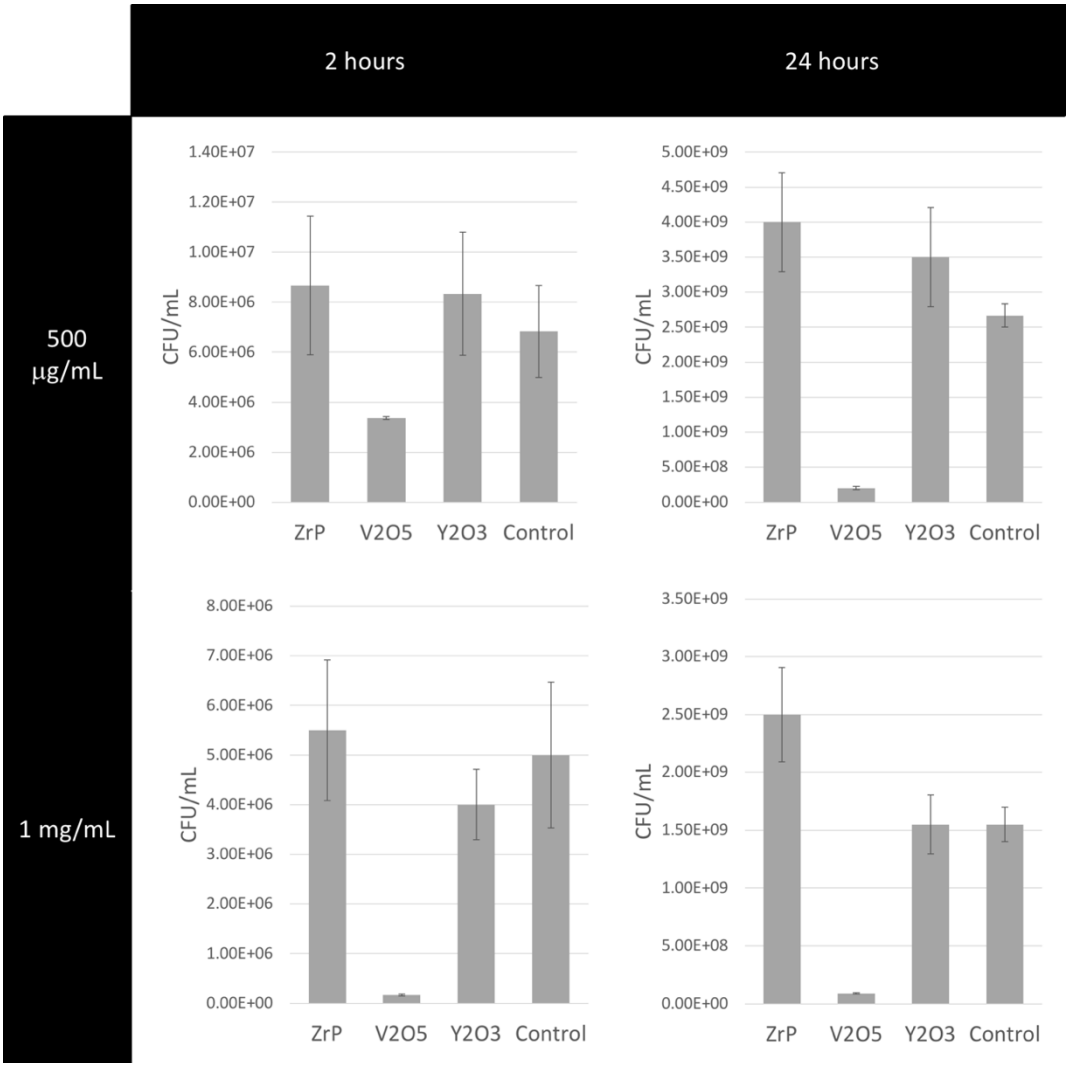

Figure 15: Plots showing the results for various nanoparticles cultured with *S. aureus*.

The antibacterial effect was calculated with the formula:

$$\text{Percent killing} = \frac{\text{control} - \text{test}}{\text{control}} * 100$$

A positive value indicates a reduction in bacteria compared to the control. 90% killing indicates a one-log reduction, while 99% killing indicates a two-log reduction, and so forth.

500 µg/mL, 2hours	Avg (CFU/mL)	Std Dev	p-value	Percent Killing
ZrP	8.67E+06	2.78E+06	0.486	-26.8%
V_2O_5	3.37E+06	6.24E+04	0.117	**50.7%**
Y_2O_3	8.33E+06	2.46E+06	0.531	-22.0%
Control	6.83E+06	1.84E+06	1	

500 µg/mL, 24 hours	Avg	Std Dev	p-value	Percent Killing
ZrP	4.00E+09	7.07E+08	0.110	-50.0%
V_2O_5	2.02E+08	2.25E+07	0.002	**92.4%**
Y_2O_3	3.50E+09	7.07E+08	0.234	-31.3%
Control	2.67E+09	1.65E+08	1	

1 mg/mL, 2 hours	Avg	Std Dev	p-value	Percent Killing
ZrP	5.50E+06	1.41E+06	0.747	-10.0%
V_2O_5	1.63E+05	1.93E+04	0.043	**96.7%**
Y_2O_3	4.00E+06	7.07E+05	0.453	20.0%
Control	5.00E+06	1.47E+06	1	

1 mg/mL, 24 hours	Avg	Std Dev	p-value	Percent Killing
ZrP	2.50E+09	4.08E+08	0.068	-61.3%
V_2O_5	8.83E+07	6.24E+06	0.005	**94.3%**
Y_2O_3	1.55E+09	2.55E+08	1	0.0%
Control	1.55E+09	1.47E+08	1	

Table 4: Nanoparticle and *S. aureus* culture results. Results are quantified in CFU/mL. A two-tailed t test for unequal variances was used, with significance determined with a p value <0.05. Tests were performed in triplicate.

5.4 Summary

This research shows potential viability of V_2O_5 nanoparticles in treating bacteria. There are, however, many variables that need to be considered before moving forward

with this project. Determining MIC through several tests of different concentrations and time periods is a possible next step. More importantly, toxicity testing of V_2O_5 nanoparticles and imaging to determine possible mechanisms should be undertaken. Nanotechnology can have unintended consequences due to the lack of understanding of how nanoparticles interact with the environment, wildlife, and the human body, and further testing should be completed before potential applications can be identified. Different types of bacteria could also be tested, such as gram-negative model organisms *E. coli and P. aeruginosa*. These subsequent tests, coupled with microscopy, may help determine and understand the treatment mechanisms. Despite the need for further understanding before applications can be developed, this research sets a baseline to the potential of V_2O_5 nanoparticles as a treatment for bacteria.

Future work includes the development of potential applications for the treatment. These applications will most likely have an industrial focus due to the toxicity seen in V_2O_5 powder. TEM imaging to view the interactions between the V_2O_5 would also be valuable to predict the mechanism of treatment. This research also indicates that 2-dimension V_2O_5 nanomaterials as a whole may have a potential for treatment against bacteria, which sets the foundation for the work in the next chapter.

CHAPTER VI

EFFECTS OF A V_2O_5-BASED NANOSTRUCTURE ON BACTERIA

This chapter discusses the treatment of methicillin-resistant *S. aureus* with a nickel-V_2O_5 nanocomposite. Experiments were performed *in vitro* at the Texas A&M Health Science Center. Methods were developed to test potential antibacterial surfaces against bacteria cultured in liquid media. Major results showed a 99.1% reduction in bacteria with a V_2O_5-nanocomposite compared to the control after 24-hours of treatment. This reduction was not seen however after two hours of treatment. SEM imaging shows both the bacteria cells and the nanocomposite after testing, but resolution and material preparation difficulties did not allow for the *S. aureus* morphology of the control sample to be compared to the bacteria cultured with the nickel-V_2O_5 nanocomposite.

This experiment also showed that morphology of the V_2O_5 nanostructure was very important in the antibacterial effects. An alternate morphology of Ni/V_2O_5 (as fabricated in Chapter 4) was tested with *S. aureus*, which did not reduce the bacterial load significantly after either 2- or 24-hours of treatment.

6.1 V_2O_5 Nanocomposite

The Ni/V_2O_5 nanocomposite tested and shown to be effective has a flower-like morphology of V_2O_5 nanosheets of a nickel substrate. SEM images can be seen in literature [47]. The purpose of this work was to show the viability of using a V_2O_5-based nanocomposite as a treatment against *S. aureus*. The first step of the experimental process was to develop testing methods to test the antibacterial surface with bacteria cultured in liquid LB. A control experiment was performed to validate the consistency of the testing protocol. The next step was to show the effectiveness of the fabricated V_2O_5 nanocomposite against *S. aureus*.

A main point of consideration was how to compare and analyze the results. There is not a baseline for antibacterial surface effectiveness, and comparing the nanostructure to just a positive, liquid-only control is problematic due to possible effects from the substrate (as the nanostructure is the main item of interest). After deliberation, a methodology was devised. A cleaned sample of the substrate would be used for the control. This would allow the percent reduction to be calculated, and nanocomposites with different substrate materials could be compared.

6.2 Cell Culture

S. aureus Xen36 was selected as the bacteria for this experiment. *S. aureus* is a common gram-positive bacterium used for *in vitro* study. The Xen36 strain contains a copy of the *Photorhabdus luminescens* lux operon, which gives the bacteria bioluminescence [68]. This allows for real-time monitoring of the bacterial load during luminescence assays. Bacteria was cultured in liquid media in 12 well tissue plates and incubated with shaking.

1) Care was used in handling the samples and were moved by holding them on the edge with forceps.
2) *S. aureus* Xen36 was inoculated into liquid LB and incubated overnight. The concentration was determined with a Nanodrop spectrophotometer and diluted to a starting concentration of 10^3 CFU/mL with liquid LB.
3) Samples (approximately 1cm x 1cm in dimension) were sterilized in 70% ethanol for 30 minutes. The samples were let dry completely in a biosafety cabinet to minimize contamination.
4) After drying, each sample was placed in a well of a 12 well tissue culture plate.
5) Two mL of the bacteria liquid culture was deposited in each well (enough to fully cover sample).

6) The well plate was covered and placed on the shaking incubator with the well taped to the shaker for security. The shaker was set to 110 rpm with an incubation time of two or 24 hours.
7) When the incubation period was finished, the samples were removed from the incubator and were testing for luminescence. Results were quantified in CPS (counts per second). Three measurements were taken for each well and the results were recorded.
8) Based on the luminescence results, the CFU/mL was tested using serial dilutions and plate counting. 100 μL was deposited for three different concentrations (ranging from neat to 10^9) onto LB agar plates. Three depositions were performed for each concentration for each sample. These plates were incubated overnight before counting the plates.
9) Samples for each liquid culture were fixed for further analysis. SEM and optical microscopy were used to analyze the resulting bacteria cell morphology and thereby predict the treatment mechanism.

6.3 Results

Luminescence Testing

Results were quantified with luminescence testing in counts/second (CPS). Initial testing during the development of the experimental methods were performed and showed a linear trend with CFU/mL and CPS with this. Future testing should confirm that data with CFU results.

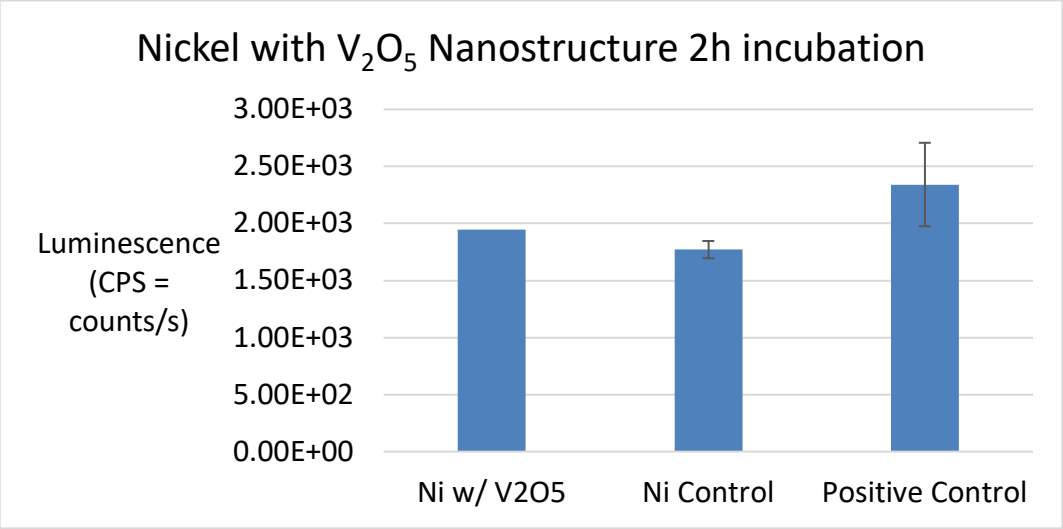

Figure 16: Results of the bacteria testing with V_2O_5 nanocomposite after 2

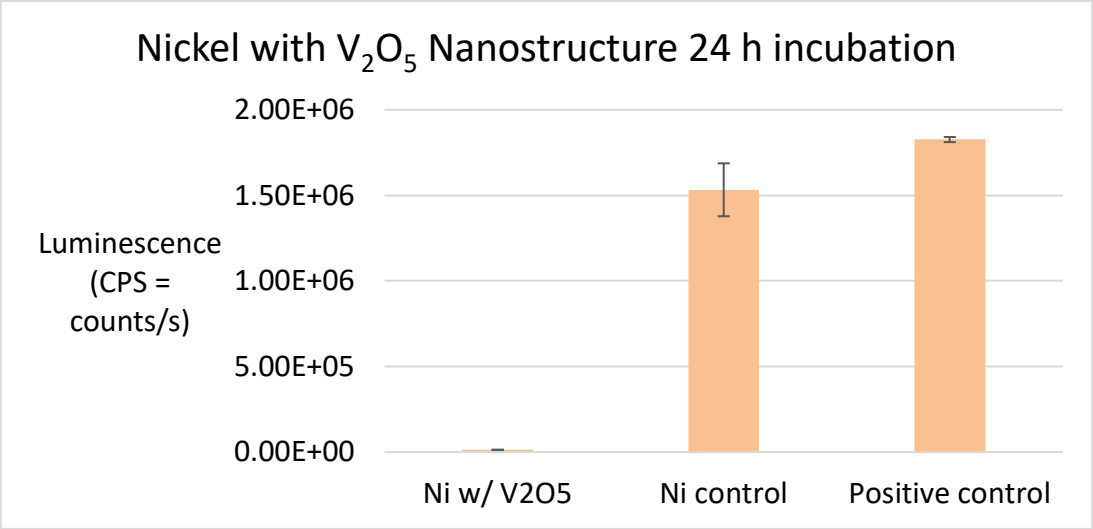

Figure 17: Results of the bacteria testing with V_2O_5 nanocomposite after 24 hours.

2-hour incubation	Average	Std Dev	Percent killing
Ni w/ V_2O_5 nanostructure	1.94E+03		-9.79%
Ni control	1.77E+03	7.56E+01	
Positive control	2.34E+03	3.66E+02	
24-hour incubation	**Average**	**Std Dev**	**Percent killing**
Ni w/ V_2O_5 nanostructure	1.36E+04	2.74E+02	99.11%
Ni control	1.53E+06	1.55E+05	
Positive control	1.83E+06	1.49E+04	

Table 6: Results of the bacteria cultured with V_2O_5 nanocomposite after 2 and 24 hours of treatment

Imaging

After testing, the sample were prepared for SEM imaging. Liquid LB containing bacteria was removed from the culture, fixed with glutaraldehyde, and dehydrated with an ethanol series before imaging. Images of *S. aureus* for the control and test samples are seen below in Figures 18 and 19. Difficulties in obtaining a sufficient resolution did not allow the morphology of the bacteria cells to be compared as rigorously as desired. The blurry imaging (particularly in Figure 19) may be caused by insufficient drying during the fixation process. The shape and size of the individual cells can be in Figure 18. Further imaging should be completed in the future, with particular consideration on the fixing and dehydrating processes.

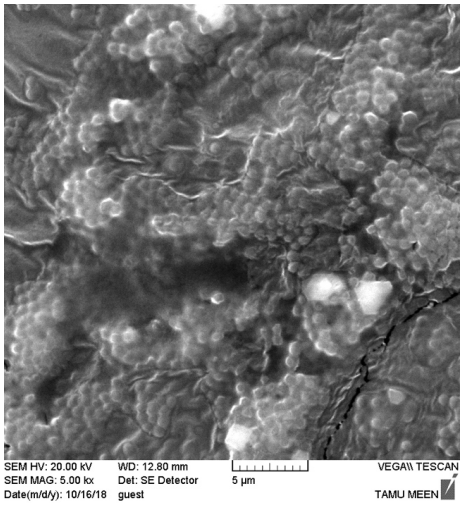

Figure 18: SEM imaging of *S. aureus* after incubation for 2 hours. Bacteria was fixed with a glutaraldehyde solution and dehydrated with ethanol before imaging.

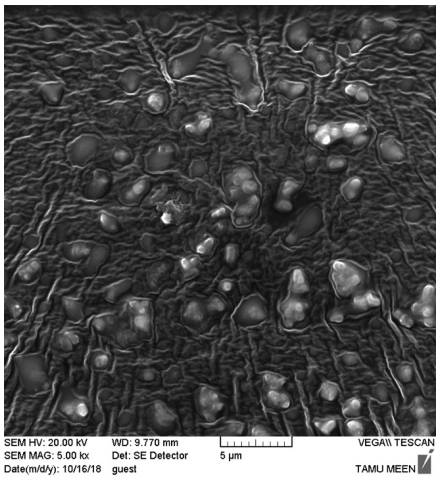

Figure 20: SEM imaging of bacteria in the liquid LB cultured with the Ni/V2O5 nanocomposite.

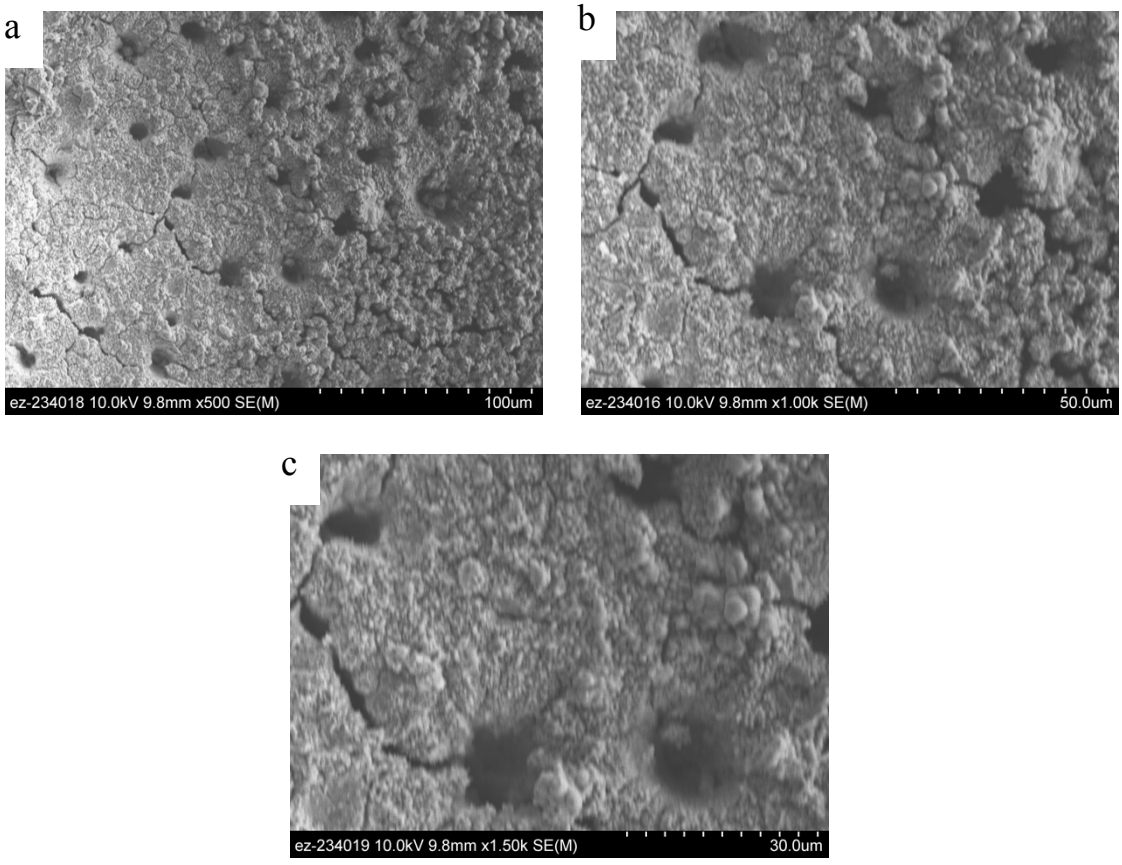

Figure 19: SEM imaging of the Ni/V_2O_5 nanocomposite after incubation with *S. aureus* at magnifications of (a) 500x, (b) 1000x, and (c) 1500x.

SEM of the Ni/V_2O_5 nanocomposite is seen above in Figure 19. Similar to Figures 27 and 28, the resolution was not high enough to determine if individual *S. aureus* cells were left on the surface after the fixing and dehydrating process.

SEM imaging of the samples did not yield conclusive details about the bacteria and material interactions. Magnifications of higher than 1500x did not yield images of high resolution. The method of preparing the samples for imaging (fixing with a glutaraldehyde solution and dehydrating with ethanol) could also be an issue. Future work involving higher resolution imaging (either with different SEM equipment or with better material preparation) is key to predicting the bacteria-material interactions.

6.4 Discussion

A total of eight experiments were performed in the development of the experimental methods. Initially, the samples were incubation without shaking. Shaking was added after the first experiment to possibly increase the amount of interaction between the bacteria and the nanostructure surface and to increase the consistency of the results. The shaking machine can be seen in Figure 21. This shaking facilitated the testing of the stability of the coating in liquid LB. This led to the removal of one of the substrate materials from the testing pool, as discussed later.

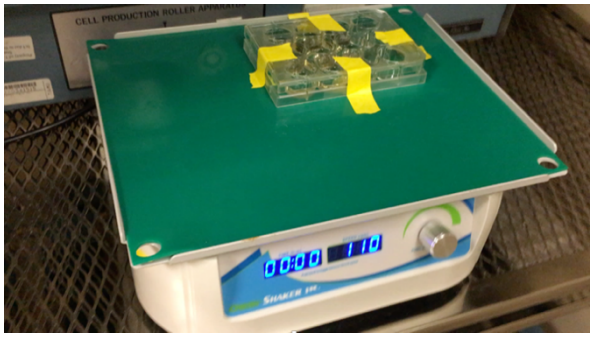

Figure 21: Well plate incubating on a shaker

Picking the ideal tissue well size was an important part of the methods development. Initially, 6-well tissue culture plates were used. These wells were 34.8mm in diameter and a well volume of 16.8mL (Sigma-Aldrich). Results from the first test were

inconsistent (Figure 23), and well size was identified as a possible cause due to drying out of the samples during tested. Well size was switched to a 12-well tissue plate which had a smaller well volume of 22.1mm and a well volume of 6.9mL. Well size is compared in Figure 22. The goal was to lower the surface area of the liquid and decrease the drying out of the sample, which would then hopefully lead to more consistent results.

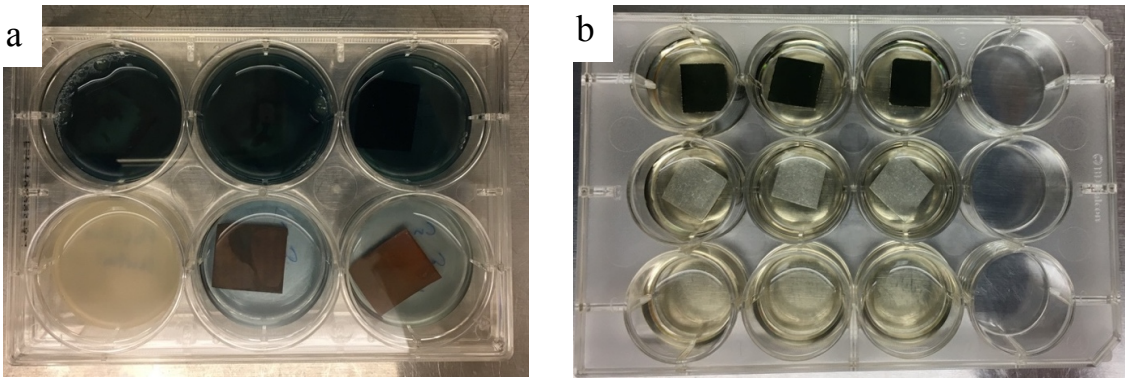

Figure 22: Images comparing the different well sizes used (a) 6 well plate and (b) 12 well plate. Coating coming off from the copper substrate can also be seen in all three samples on the top row in (a)

Figure 23: Plot showing the inconsistency in the 6 well plate. Notice the large standard deviation in the copper control compared to the mean. Conclusions cannot be drawn from this data due to the inconsistency of the control.

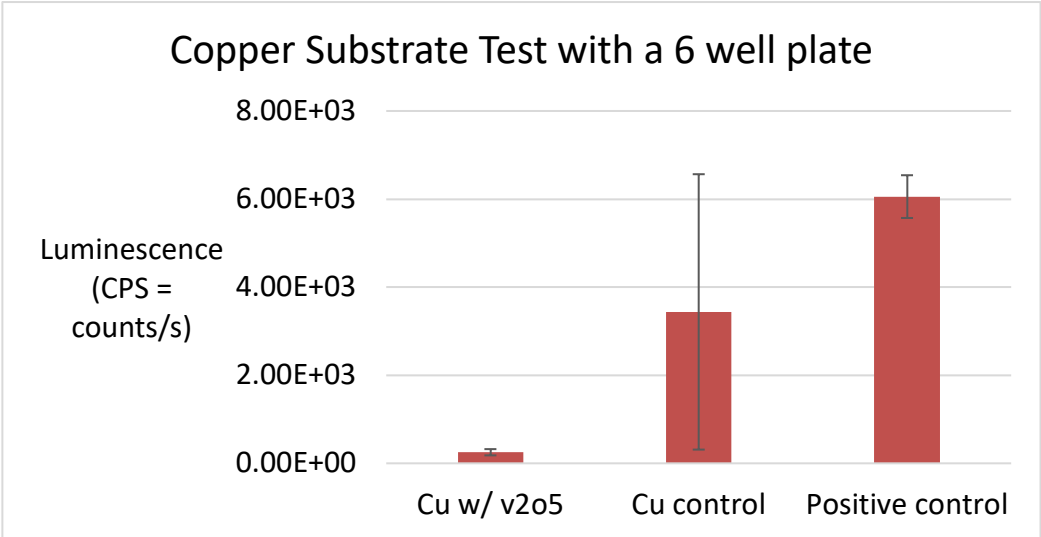

Coating durability was also an area of concern. As seen in Chapter 4, the copper sample prepped with sanding resulted in a consistent surface coating. However, when tested in liquid LB with shaking, the coating was not durable and leached into the liquid (as seen in Figure 22 and 24). Copper was eliminated from the testing pool due to this issue. This issue was also the case for some of the aluminum samples (Figure 24). Aluminum was also eliminated as a potential substrate partially due to this issue.

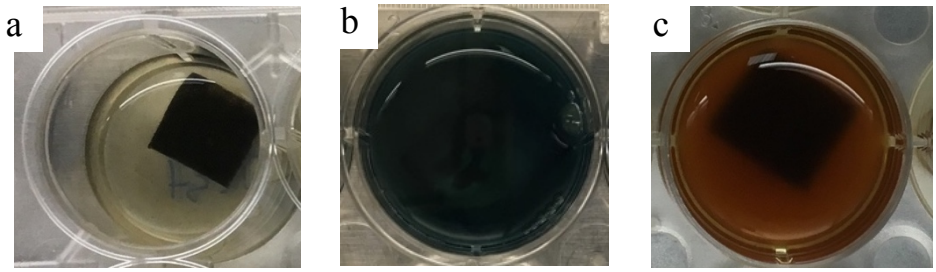

Figure 24: Image of (a) Ni-V_2O_5, (b) Cu-V_2O_5, and (c) Al-V_2O_5 in liquid LB cultured with *S. aureus* after 24 hours of incubation with. The coatings on the Cu-V_2O_5 and the Al-V_2O_5 samples were not durable and came off/leached into the liquid LB. The coating on the nickel substrate was much more durable and did not visibility come off/leach into the liquid.

Incubation time is also important. Differences, particularly for the Ni/V_2O_5 sample prepared with electrodeposition with the carbon rod, are notable. This sample showed a 99.1% reduction in bacteria compared to the control over 24 hours, but no reduction was seen at the 2-hour time point. Testing multiple incubation times in important for future work. Multiple data points will allow a curve to be established and for the mechanism to be better understood. Incubation time results can also affect the potential applications for this treatment.

Control Experiment

As discussed in the methods section of this chapter, a control experiment was run to validate the consistency of the control samples. This data from the control reinforced

the confidence in the validity of the testing protocol, specifically after the previously variables were adjusted (shaking, well size, triplicate testing). Samples of the nickel control and the aluminum control, as well as the positive liquid-only controls, were testing to validate the consistency. Experimental setup is seen in Figure 25 with the results of the experiment in Figure 26. The means of the controls were similar within their materials. The aluminum control showed a strong antibacterial effect in comparison to the other controls. The nickel, however, had similar CPS values to the positive control with small standard deviations.

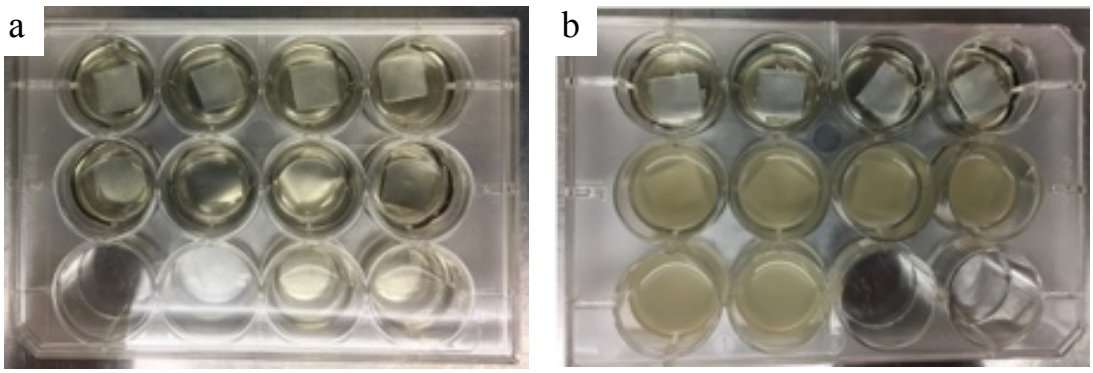

Figure 25: Control experiment with aluminum 6061 (top row) and nickel substrates (second row), (a) before incubation and (b) after incubation. The positive control is in the third row in both photos.

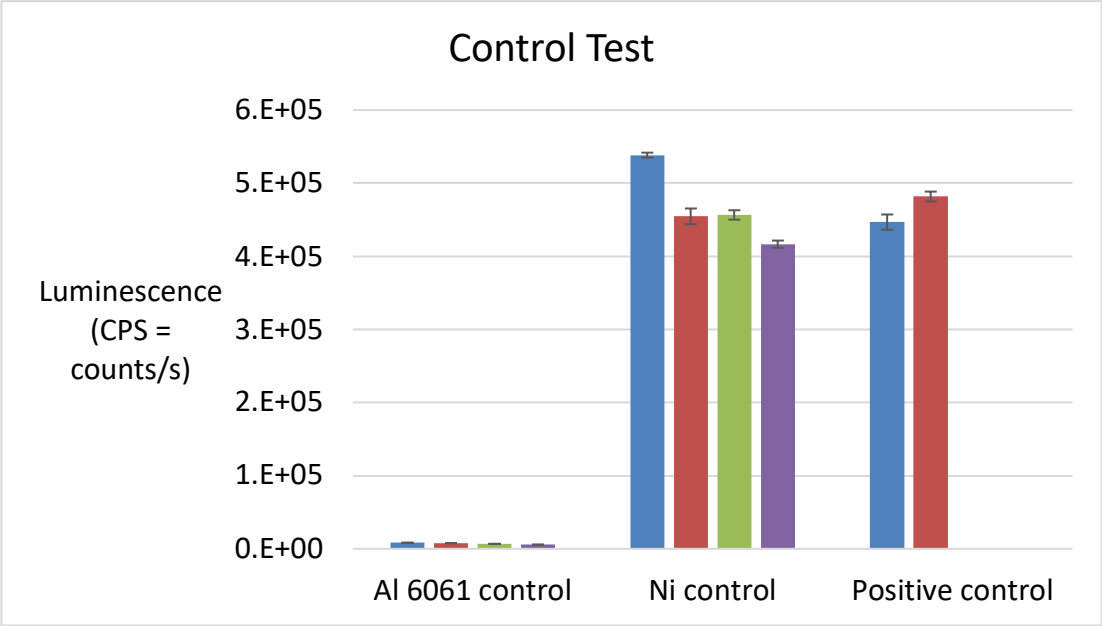

Figure 26: Control experiment with aluminum and nickel substrate, along with a positive control without a substrate.

Due to the results from the control experiment, the composition of the substrates, particularly the aluminum samples, were also scrutinized. The aluminum substrate was 6061 aluminum, which contains trace amounts of copper (0.4%) and other elements (see Chapter 4 for more information on substrate composition). This copper in the material may be having an antibacterial effect during the experiment and may be affecting the results. We decided to focus on the nickel substrate after this test. Possible future testing and fabrication could use an aluminum alloy that does not contain copper.

Nanostructure Morphology

2-hour incubation	Percent killing
Ni w/ V_2O_5 sample 1	-9.8%
Ni w/ V_2O_5 sample 2	20.7%
24-hour incubation	**Percent killing**
Ni w/ V_2O_5 sample 1	99.1%
Ni w/ V_2O_5 sample 2	-253.1%

Table 7: The results above show the difference in antibacterial activity for the two different Ni/V2O5 nanocomposite morphologies. The different morphologies can be seen in literature for sample 1 and in Figure 9 for sample 2 [47]. Negative values indicate increased growth and positive values indicate reduction in comparison to the control.

The results for the different morphologies are significant. One morphology yielded a 99.1% reduction, while the other lead to increases of over 250% in comparison to the control. While this is still just an initial viability test, future testing should be conducted, particularly with multiple samples and after 2 and 24 hours of treatment.

Possible Mechanisms

Multiple mechanisms could be accounting for the antibacterial effects seen for the nanostructured V_2O_2 on nickel substrate. One such proposed mechanism for the antibacterial effect of the is illustrated below in Figure 27. This mechanism is similar to that of the graphene nanosheets and E. coli discussed in detail in Chapter 1. The sharp edges and morphology of the deposited nanosheets could be damaging the cell wall of the bacteria, causing leakage of intracellular components out of the cell. This mechanism has been shown in literature for nanoparticles with a similar morphology to the fabricated V_2O_5 nanomaterials discussed in this research [41], but the mechanism has not been seen or applied for antibacterial surfaces.

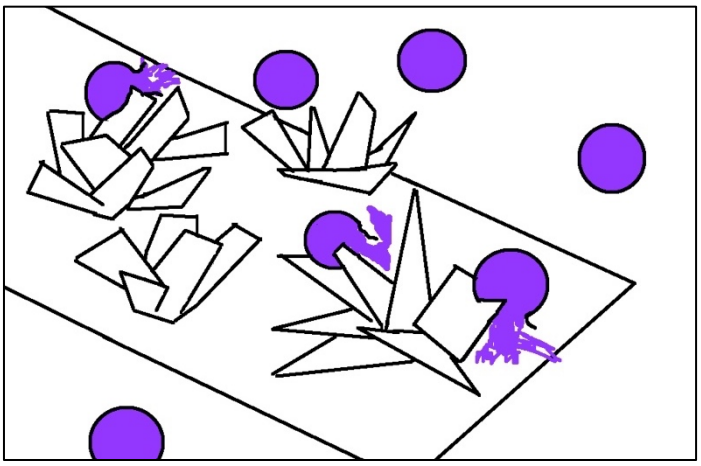

Figure 27: One of the proposed mechanisms for the antibacterial effect of Ni/V_2O_5 nanocomposite. The sharp edges of the deposited nanosheets cut through the cell wall and lead to leakage of intracellular components

Other proposed mechanisms include reduced adhesion to the surface [69], disruption of the permeability of the cellular membrane [70], and formation of reactive oxygen species (ROS) [71], all of which have been shown for other antibacterial nanomaterials.

6.5 Summary

This research shows the viability of using a V_2O_5 nanocomposite surface in treating bacteria. Effective treatment was show over 24-hour time periods. SEM imaging of both *S. aureus* controls and those incubated with the Ni/V_2O_5 nanocomposite were inconclusive for validating potential mechanisms. Greater imaging resolution and better material preparation is needed for higher quality imaging of bacteria morphology. Further imaging may allow for a more accurate prediction of a possible mechanism of treatment. A proposed mechanism for the material-bacteria interaction involving damage to the bacteria membrane and leakage of intercellular components out of the cell is illustrated and presented.

Future work should further replicate and confirm the antibacterial effect after various times of treatment. This would further allow the mechanism to be studied and to understand the difference between the 2- and 24-hour incubation periods. This will help development a trend for the amount of time needed for effective bacteria reduction and will further shed light on the treatment mechanism. This project would also benefit from multiple trials of the same experiment to validate consistency of the data.

CHAPTER VII
CONCLUSIONS AND FUTURE RESEARCH

Antibacterial nanomaterials are an important area of current research due to potential new methods and physical mechanisms of treatment. These antibacterial nanomaterials have a wide range of potential applications, including manufacturing, water treatment, oil/gas, and biomedicine. Several nanoparticles and nanostructures were fabricated using a variety of substrate materials, surface treatments, and coating generation methods. Bacterium *S. aureus* was tested with the fabricated nanoparticles and nanostructures. The inserted bioluminescence lux operon in the strain used (*S. aureus* Xen36) allowed for quick determinations of the bacterial loads. Following bacteria testing and microscopic analysis, V_2O_5 nanomaterials were shown to have potential as antibacterial agents.

The major findings are summarized in the following.

1. The nanoparticles of V_2O_5 showed potential for antibacterial treatment. Results indicated that they are effective after 2 and 24-hours of treatment when tested *in vivo* against *S. aureus*, with a decrease in bacterial load of 92.4%, 96.7%, and 94.3% at concentrations of 500ug/mL for 24 hours, 1mg/mL for 2 hours, and 1mg/mL for 24 hours, respectively. In addition, the Ni/V_2O_5 nanocomposite caused a 99.1% decrease in bacterial load in comparison to the control.
2. Nanostructured materials, including a Ni sheet deposited with nanostructured V_2O_5, were evaluated with *S. aureus.* Results showed that the V_2O_5 nanostructured surfaces with sharp morphological characteristic do not promote cell proliferation. A physical model was proposed that the sharp morphology of the deposited V_2O_5 nanosheets may be damaging the cell wall of cells and causing lysis.

Multiple future recommendations for expanded research and study remain:

- The mechanism of treatment is also difficult to study without high quality electron microscopy. Bacteria morphology, particularly differences between the control samples and effective test samples will give hints towards the mechanism of treatment. Both individual cells and the interaction between the nanostructure and the cells should be imaged. Resolution of the images needs to be high in order to see these interactions. Multiple incubation time points and nanostructure morphologies should be studied. This will further allow the bacteriostatic and/or bactericidal effects of the materials to be studied.
- Nanostructure durability is also an area of concern. Both the copper and aluminum substrates resulted in their coating coming off into the LB liquid during incubation. This was minimized in for the nickel substrates; however, this was not rigorously tested with quantitative analysis. Future testing could add comparing the weights of the nanocomposite before and after incubation to determine if any leaching of the coatings into the liquid or corrosion took place. The LB liquid could also be checked for the presence of V_2O_5 materials that came off of the nanocomposite. Improving the durability by preventing the leaching is also important is producing a reusable and environmentally friendly antibacterial surface. It is also important to show the mechanism of treatment, as the mechanism is not yet fully understood.
- Future testing can also study different types of bacteria, including gram-negative and mycobacteria species. Showing effective treatment over a wide range of bacteria species could expand potential future applications and increase interest in the use of V_2O_5 nanomaterials for bacteria treatment. Further toxicity testing for V_2O_5 nanomaterials is also lacking. Without this nanotoxicity data, use of these treatment methods may not be worth the risk due to potential health risks and environmental exposure.

REFERENCES

1. Lee, H., S.Y. Yeo, and S.H. Jeong, *Antibacterial effect of nanosized silver colloidal solution on textile fabrics.* Journal of Materials Science, 2003. **38**(10): p. 2199-2204.

2. Hu, W., et al., *Graphene-based antibacterial paper.* ACS nano, 2010. **4**(7): p. 4317-4323.

3. Li, Q., et al., *Antimicrobial nanomaterials for water disinfection and microbial control: potential applications and implications.* Water research, 2008. **42**(18): p. 4591-4602.

4. Kulshrestha, S., et al., *A graphene/zinc oxide nanocomposite film protects dental implant surfaces against cariogenic Streptococcus mutans.* Biofouling, 2014. **30**(10): p. 1281-1294.

5. Brady-Estévez, A.S., S. Kang, and M. Elimelech, *A single-walled-carbon-nanotube filter for removal of viral and bacterial pathogens.* Small, 2008. **4**(4): p. 481-484.

6. He, J., et al., *Killing dental pathogens using antibacterial graphene oxide.* ACS applied materials & interfaces, 2015. **7**(9): p. 5605-5611.

7. Lu, Z., et al., *Size-dependent antibacterial activities of silver nanoparticles against oral anaerobic pathogenic bacteria.* Journal of Materials Science: Materials in Medicine, 2013. **24**(6): p. 1465-1471.

8. Rai, M., et al., *Silver nanoparticles: the powerful nanoweapon against multidrug-resistant bacteria.* Journal of applied microbiology, 2012. **112**(5): p. 841-852.

9. Rai, M., A. Yadav, and A. Gade, *Silver nanoparticles as a new generation of antimicrobials.* Biotechnology advances, 2009. **27**(1): p. 76-83.

10. Wu, J., et al., *In situ synthesis of silver-nanoparticles/bacterial cellulose composites for slow-released antimicrobial wound dressing.* Carbohydrate polymers, 2014. **102**: p. 762-771.

11. Maneerung, T., S. Tokura, and R. Rujiravanit, *Impregnation of silver nanoparticles into bacterial cellulose for antimicrobial wound dressing.* Carbohydrate polymers, 2008. **72**(1): p. 43-51.

12. Raffi, M., et al., *Investigations into the antibacterial behavior of copper nanoparticles against Escherichia coli.* Annals of microbiology, 2010. **60**(1): p. 75-80.

13. Raghupathi, K.R., R.T. Koodali, and A.C. Manna, *Size-dependent bacterial growth inhibition and mechanism of antibacterial activity of zinc oxide nanoparticles.* Langmuir, 2011. **27**(7): p. 4020-4028.

14. Zharov, V.P., et al., *Photothermal nanotherapeutics and nanodiagnostics for selective killing of bacteria targeted with gold nanoparticles.* Biophysical journal, 2006. **90**(2): p. 619-627.

15. He, S., et al., *Biosynthesis of gold nanoparticles using the bacteria Rhodopseudomonas capsulata.* Materials Letters, 2007. **61**(18): p. 3984-3987.

16. Husseiny, M., et al., *Biosynthesis of gold nanoparticles using Pseudomonas aeruginosa.* Spectrochimica Acta Part A: Molecular and Biomolecular Spectroscopy, 2007. **67**(3-4): p. 1003-1006.

17. Zhao, Y., et al., *Small molecule-capped gold nanoparticles as potent antibacterial agents that target gram-negative bacteria.* Journal of the American Chemical Society, 2010. **132**(35): p. 12349-12356.

18. Jayakumar, R., et al., *Biomedical applications of chitin and chitosan based nanomaterials—A short review.* Carbohydrate Polymers, 2010. **82**(2): p. 227-232.

19. Banoee, M., et al., *ZnO nanoparticles enhanced antibacterial activity of ciprofloxacin against Staphylococcus aureus and Escherichia coli.* Journal of Biomedical Materials Research Part B: Applied Biomaterials, 2010. **93**(2): p. 557-561.

20. Rajasree, S.R. and T. Suman, *Extracellular biosynthesis of gold nanoparticles using a gram negative bacterium Pseudomonas fluorescens.* Asian Pacific Journal of Tropical Disease, 2012. **2**: p. S796-S799.

21. Hernández-Sierra, J.F., et al., *The antimicrobial sensitivity of Streptococcus mutans to nanoparticles of silver, zinc oxide, and gold.* Nanomedicine: Nanotechnology, Biology and Medicine, 2008. **4**(3): p. 237-240.

22. Jones, N., et al., *Antibacterial activity of ZnO nanoparticle suspensions on a broad spectrum of microorganisms.* FEMS microbiology letters, 2008. **279**(1): p. 71-76.

23. Nanda, A. and M. Saravanan, *Biosynthesis of silver nanoparticles from Staphylococcus aureus and its antimicrobial activity against MRSA and MRSE.* Nanomedicine: Nanotechnology, Biology and Medicine, 2009. **5**(4): p. 452-456.

24. Gupta, R.S., *Protein phylogenies and signature sequences: a reappraisal of evolutionary relationships among archaebacteria, eubacteria, and eukaryotes.* Microbiology and Molecular Biology Reviews, 1998. **62**(4): p. 1435-1491.

25. Passman, F.J., *Controlling microbial contamination in metal working fluids.* TECHNICAL PAPERS-SOCIETY OF MANUFACTURING ENGINEERS-ALL SERIES-, 1992.

26. Pankey, G. and L. Sabath, *Clinical relevance of bacteriostatic versus bactericidal mechanisms of action in the treatment of Gram-positive bacterial infections.* Clinical infectious diseases, 2004. **38**(6): p. 864-870.

27. McDonnell, G. and A.D. Russell, *Antiseptics and disinfectants: activity, action, and resistance.* Clinical microbiology reviews, 1999. **12**(1): p. 147-179.

28. Marquis, B.J., et al., *Analytical methods to assess nanoparticle toxicity.* Analyst, 2009. **134**(3): p. 425-439.

29. Allsopp, M., A. Walters, and D. Santillo, *Nanotechnologies and nanomaterials in electrical and electronic goods: A review of uses and health concerns.* Greenpeace Research Laboratories, London, 2007.

30. Monteiro-Riviere, N., A. Inman, and L. Zhang, *Limitations and relative utility of screening assays to assess engineered nanoparticle toxicity in a human cell line.* Toxicology and applied pharmacology, 2009. **234**(2): p. 222-235.

31. Dong, A., et al., *Barbituric acid-based magnetic N-halamine nanoparticles as recyclable antibacterial agents.* ACS applied materials & interfaces, 2013. **5**(16): p. 8125-8133.

32. Yao, Q., et al., *Surface arming magnetic nanoparticles with amine N-halamines as recyclable antibacterial agents: construction and evaluation.* Colloids and Surfaces B: Biointerfaces, 2016. **144**: p. 319-326.

33. Hunt, P.R., et al., *Bioactivity of nanosilver in Caenorhabditis elegans: Effects of size, coat, and shape.* Toxicology reports, 2014. **1**: p. 923-944.

34. Sadeghi, B., et al., *Comparison of the anti-bacterial activity on the nanosilver shapes: nanoparticles, nanorods and nanoplates.* Advanced Powder Technology, 2012. **23**(1): p. 22-26.

35. Choi, O. and Z. Hu, *Size dependent and reactive oxygen species related nanosilver toxicity to nitrifying bacteria.* Environmental science & technology, 2008. **42**(12): p. 4583-4588.

36. Zhao, L., et al., *Antibacterial nano-structured titania coating incorporated with silver nanoparticles.* Biomaterials, 2011. **32**(24): p. 5706-5716.

37. Kim, J.S., et al., *Antimicrobial effects of silver nanoparticles.* Nanomedicine: Nanotechnology, Biology and Medicine, 2007. **3**(1): p. 95-101.

38. Hui, L., et al., *Availability of the basal planes of graphene oxide determines whether it is antibacterial.* ACS applied materials & interfaces, 2014. **6**(15): p. 13183-13190.

39. Liu, S., et al., *Lateral dimension-dependent antibacterial activity of graphene oxide sheets.* Langmuir, 2012. **28**(33): p. 12364-12372.

40. Akhavan, O. and E. Ghaderi, *Toxicity of graphene and graphene oxide nanowalls against bacteria.* ACS nano, 2010. **4**(10): p. 5731-5736.

41. Tu, Y., et al., *Destructive extraction of phospholipids from Escherichia coli membranes by graphene nanosheets.* Nature nanotechnology, 2013. **8**(8): p. 594.

42. Christenson, E.M., et al., *Nanobiomaterial applications in orthopedics.* Journal of Orthopaedic Research, 2007. **25**(1): p. 11-22.

43. Jiang, H., et al., *Plasma-enhanced deposition of silver nanoparticles onto polymer and metal surfaces for the generation of antimicrobial characteristics.* Journal of Applied Polymer Science, 2004. **93**(3): p. 1411-1422.

44. Agnihotri, S., S. Mukherji, and S. Mukherji, *Immobilized silver nanoparticles enhance contact killing and show highest efficacy: elucidation of the mechanism of bactericidal action of silver.* Nanoscale, 2013. **5**(16): p. 7328-7340.

45. Dai, W., et al., *Formation of anti-wear tribofilms via α-ZrP nanoplatelet as lubricant additives.* Lubricants, 2016. **4**(3): p. 28.

46. Howarth, O.W. and J.R. Hunt, *Peroxo-complexes of vanadium (V); a vanadium-51 nuclear magnetic resonance study.* Journal of the Chemical Society, Dalton Transactions, 1979(9): p. 1388-1391.

47. Yue, Y., et al., *Super-hierarchical Ni/porous-Ni/V 2 O 5 nanocomposites.* RSC Advances, 2017. **7**(64): p. 40383-40391.

48. Natalio, F., et al., *Vanadium pentoxide nanoparticles mimic vanadium haloperoxidases and thwart biofilm formation.* Nature nanotechnology, 2012. **7**(8): p. 530.

49. Pan, A., et al., *Facile synthesized nanorod structured vanadium pentoxide for high-rate lithium batteries.* Journal of Materials Chemistry, 2010. **20**(41): p. 9193-9199.

50. Cao, A.M., et al., *Self-assembled vanadium pentoxide (V2O5) hollow microspheres from nanorods and their application in lithium-Ion batteries.* Angewandte Chemie International Edition, 2005. **44**(28): p. 4391-4395.

51. Zhu, J., et al., *Building 3D structures of vanadium pentoxide nanosheets and application as electrodes in supercapacitors.* Nano letters, 2013. **13**(11): p. 5408-5413.

52. Muhr, H.J., et al., *Vanadium oxide nanotubes—a new flexible vanadate nanophase.* Advanced Materials, 2000. **12**(3): p. 231-234.

53. Xiong, C., et al., *Fabrication of silver vanadium oxide and V2O5 nanowires for electrochromics.* ACS nano, 2008. **2**(2): p. 293-301.

54. Li, J., et al., *Synthesis of Ag modified vanadium oxide nanotubes and their antibacterial properties.* Materials Research Bulletin, 2008. **43**(10): p. 2810-2817.

55. Masalha, M., et al., *Analysis of Transcription of theStaphylococcus aureus Aerobic Class Ib and Anaerobic Class III Ribonucleotide Reductase Genes in Response to Oxygen.* Journal of bacteriology, 2001. **183**(24): p. 7260-7272.

56. Tong, T., et al., *Effects of material morphology on the phototoxicity of nano-TiO2 to bacteria.* Environmental science & technology, 2013. **47**(21): p. 12486-12495.

57. Naimi, T.S., et al., *Comparison of community-and health care–associated methicillin-resistant Staphylococcus aureus infection.* Jama, 2003. **290**(22): p. 2976-2984.

58. Schlecht, L.M., et al., *Systemic Staphylococcus aureus infection mediated by Candida albicans hyphal invasion of mucosal tissue.* Microbiology, 2015. **161**(1): p. 168-181.

59. Weigel, L.M., et al., *Genetic analysis of a high-level vancomycin-resistant isolate of Staphylococcus aureus.* Science, 2003. **302**(5650): p. 1569-1571.

60. Sun, L., et al., *Preparation of α-zirconium phosphate nanoplatelets with wide variations in aspect ratios.* New Journal of Chemistry, 2007. **31**(1): p. 39-43.

61. Fontenot, C.J., et al., *Vanadia gel synthesis via peroxovanadate precursors. 1. in situ laser Raman and 51V NMR characterization of the gelation process.* The Journal of Physical Chemistry B, 2000. **104**(49): p. 11622-11631.

62. Liu, Y., et al., *V2O5 Nano-Electrodes with High Power and Energy Densities for Thin Film Li-Ion Batteries.* Advanced Energy Materials, 2011. **1**(2): p. 194-202.

63. Chen, Y., *Synthesis, Characterization, and Applications of Rare-Earth-Element-Doped Nanoparticles"*. 2017, ProQuest Information and Learning Company.

64. Zhang, F., et al., *Fabrication of Ag@ SiO2@ Y2O3: Er nanostructures for bioimaging: tuning of the upconversion fluorescence with silver nanoparticles.* Journal of the American Chemical Society, 2010. **132**(9): p. 2850-2851.

65. Jung, H.-Y., et al., *Enhanced electro-optical properties of Y2O3 (yttrium trioxide) nanoparticle-doped twisted nematic liquid crystal devices.* Liquid Crystals, 2012. **39**(7): p. 789-793.

66. Yu, L., et al., *Preparation and tribological properties of surface-modified nano-Y2O3 as additive in liquid paraffin.* Applied Surface Science, 2012. **263**: p. 655-659.

67. Srinivasan, R., R. Yogamalar, and A. Chandra Bose, *Synthesis and structural studies on nanocrystalline yttrium oxide.* Advanced Science Letters, 2009. **2**(1): p. 65-69.

68. *Staphylococcus aureus - Xen36*. [cited 2018; Available from: http://www.perkinelmer.com/product/xen36-staphylococcus-aureus-119243.

69. Lara, H.H., et al., *Silver nanoparticles are broad-spectrum bactericidal and virucidal compounds.* Journal of nanobiotechnology, 2011. **9**(1): p. 30.

70. Hajipour, M.J., et al., *Antibacterial properties of nanoparticles.* Trends in biotechnology, 2012. **30**(10): p. 499-511.

71. Applerot, G., et al., *ZnO nanoparticle-coated surfaces inhibit bacterial biofilm formation and increase antibiotic susceptibility.* Rsc Advances, 2012. **2**(6): p. 2314-2321.

72. Brinksmeier, E., et al., *Metalworking fluids—Mechanisms and performance.* CIRP Annals, 2015. **64**(2): p. 605-628.

73. Gauthier, S.L., *Metalworking fluids: oil mist and beyond.* Applied occupational and environmental hygiene, 2003. **18**(11): p. 818-824.

74. Astakhov, V.P. and S. Joksch, *Metalworking fluids (MWFs) for cutting and grinding: Fundamentals and recent advances*. 2012: Elsevier.

75. Saha, R. and R.S. Donofrio, *The microbiology of metalworking fluids.* Applied microbiology and biotechnology, 2012. **94**(5): p. 1119-1130.

76. Kreiss, K. and J. Cox-Ganser, *Metalworking fluid-associated hypersensitivity pneumonitis: a workshop summary.* American journal of industrial medicine, 1997. **32**(4): p. 423-432.

77. Childers, J.C., *The chemistry of metalworking fluids.* MANUFACTURING ENGINEERING AND MATERIALS PROCESSING, 1994. **41**: p. 165-165.

78. Perkins, S.D. and L.T. Angenent, *Potential pathogenic bacteria in metalworking fluids and aerosols from a machining facility.* FEMS microbiology ecology, 2010. **74**(3): p. 643-654.

79. Simpson, A., et al., *Occupational exposure to metalworking fluid mist and sump fluid contaminants.* Annals of Occupational Hygiene, 2003. **47**(1): p. 17-30.

80. Sheehan, M.J., *Final report of the OSHA metalworking fluids standards advisory committee.* US Department of Labor, Occupational Safety and Health Administrations, Washington, DC, 1999.

81. Directive, E., *98/8/EC of the European Parliament and of the Council of 16 February 1998 concerning the placing of biocidal products on the market.* Official J. L, 1998. **123**: p. 1-63.

82. Whittaker, S.G., *Metalworking Fluids: A Resource for Employers and Health & Safety Personnel in Washington State*. 1997: Safety and Health Assessment and Research for Prevention, Washington State Department of Labor & Industries.

83. Rossmoore, H., *Antimicrobial agents for water-based metalworking fluids.* Journal of Occupational and Environmental Medicine, 1981. **23**(4): p. 247-254.

84. Foxall-VanAken, S., et al., *Common components of industrial metal-working fluids as sources of carbon for bacterial growth.* Applied and environmental microbiology, 1986. **51**(6): p. 1165-1169.

85. Mattsby-Baltzer, I., et al., *Microbial growth and accumulation in industrial metal-working fluids.* Applied and Environmental Microbiology, 1989. **55**(10): p. 2681-2689.

86. Van Der Gast, C.J., et al., *Bacterial community structure and function in a metal-working fluid.* Environmental Microbiology, 2003. **5**(6): p. 453-461.

87. Gilbert, Y., M. Veillette, and C. Duchaine, *Metalworking fluids biodiversity characterization.* Journal of applied microbiology, 2010. **108**(2): p. 437-449.

88. Livermore, D.M., *Multiple mechanisms of antimicrobial resistance in Pseudomonas aeruginosa: our worst nightmare?* Clinical infectious diseases, 2002. **34**(5): p. 634-640.

89. O'toole, G.A. and R. Kolter, *Flagellar and twitching motility are necessary for Pseudomonas aeruginosa biofilm development.* Molecular microbiology, 1998. **30**(2): p. 295-304.

90. Murat, J.-B., et al., *Factors influencing the microbial composition of metalworking fluids and potential implications for machine operator's lung.* Applied and environmental microbiology, 2012. **78**(1): p. 34-41.

91. Wallace Jr, R.J., et al., *Presence of a single genotype of the newly described species Mycobacterium immunogenum in industrial metalworking fluids associated with hypersensitivity pneumonitis.* Applied and Environmental Microbiology, 2002. **68**(11): p. 5580-5584.

92. Rosenman, K.D., *Asthma, hypersensitivity pneumonitis and other respiratory diseases caused by metalworking fluids.* Current opinion in allergy and clinical immunology, 2009. **9**(2): p. 97-102.

93. Greaves, I.A., et al., *Respiratory health of automobile workers exposed to metal-working fluid aerosols: respiratory symptoms.* American journal of industrial medicine, 1997. **32**(5): p. 450-459.

94. De Groote, M.A. and G. Huitt, *Infections due to rapidly growing mycobacteria.* Clinical infectious diseases, 2006. **42**(12): p. 1756-1763.

95. Selvaraju, S.B., I.U. Khan, and J.S. Yadav, *Biocidal activity of formaldehyde and nonformaldehyde biocides toward Mycobacterium immunogenum and Pseudomonas fluorescens in pure and mixed suspensions in synthetic metalworking fluid and saline.* Applied and environmental microbiology, 2005. **71**(1): p. 542-546.

96. Fariñas, M. and L. Martínez-Martínez, *Multiresistant Gram-negative bacterial infections: Enterobacteria, Pseudomonas aeruginosa, Acinetobacter baumannii and other non-fermenting Gram-negative bacilli.* Enfermedades infecciosas y microbiologia clinica, 2013. **31**(6): p. 402-409.

97. Hsueh, P.-R., et al., *Outbreak of Pseudomonas fluorescensbacteremia among oncology patients.* Journal of clinical microbiology, 1998. **36**(10): p. 2914-2917.

98. Cyprowski, M., et al., *Microbial and endotoxin contamination of water-soluble metalworking fluids.* International journal of occupational medicine and environmental health, 2007. **20**(4): p. 365-371.

99. Khashe, S. and J.M. Janda, *Biochemical and Pathogenic Properties ofShewanella alga and Shewanella putrefaciens.* Journal of clinical microbiology, 1998. **36**(3): p. 783-787.

100. Breidenstein, E.B., C. de la Fuente-Núñez, and R.E. Hancock, *Pseudomonas aeruginosa: all roads lead to resistance.* Trends in microbiology, 2011. **19**(8): p. 419-426.

101. Hall, C.W. and T.-F. Mah, *Molecular mechanisms of biofilm-based antibiotic resistance and tolerance in pathogenic bacteria.* FEMS microbiology reviews, 2017. **41**(3): p. 276-301.

102. Trafny, E.A., et al., *Microbial contamination and biofilms on machines of metal industry using metalworking fluids with or without biocides.* International Biodeterioration & Biodegradation, 2015. **99**: p. 31-38.

103. Trafny, E.A., et al., *Use of MTT assay for determination of the biofilm formation capacity of microorganisms in metalworking fluids.* World Journal of Microbiology and Biotechnology, 2013. **29**(9): p. 1635-1643.

104. Mullis, S.N. and J. Falkinham, *Adherence and biofilm formation of Mycobacterium avium, Mycobacterium intracellulare and Mycobacterium abscessus to household plumbing materials.* Journal of applied microbiology, 2013. **115**(3): p. 908-914.

105. Canter, N., *Monitoring metalworking fluids.* Tribology & Lubrication Technology, 2011. **67**(3): p. 42.

106. Bernstein, D.I., et al., *Machine operator's lung: a hypersensitivity pneumonitis disorder associated with exposure to metalworking fluid aerosols.* Chest, 1995. **108**(3): p. 636-641.

107. Marchand, G., et al., *Evaluation of bacterial contamination and control methods in soluble metalworking fluids.* Journal of occupational and environmental hygiene, 2010. **7**(6): p. 358-366.

108. Denyer, S.P. and G. Stewart, *Mechanisms of action of disinfectants.* International biodeterioration & biodegradation, 1998. **41**(3-4): p. 261-268.

109. Poole, K., *Mechanisms of bacterial biocide and antibiotic resistance.* Journal of Applied Microbiology, 2002. **92**(s1).

110. Russell, A., *Mechanisms of bacterial resistance to non-antibiotics: Food additives and food and pharmaceutical preservatives.* Journal of Applied Microbiology, 1991. **71**(3): p. 191-201.

111. Levy, S., *Active efflux, a common mechanism for biocide and antibiotic resistance.* Journal of applied microbiology, 2002. **92**(s1).

112. *Federal Insecticide, Fungicide, and Rodenticide Act (FIFRA)*, U.S.E.P. Agency, Editor. 1910.

113. Cheng, C., D. Phipps, and R.M. Alkhaddar, *Treatment of spent metalworking fluids.* Water research, 2005. **39**(17): p. 4051-4063.

114. Dwuletzki, H., *Replacement of metalworking fluids*, in *Metalworking Fluids (MWFs) for Cutting and Grinding*. 2012, Elsevier. p. 368-388.

115. Sosnowski, P., A. Wieczorek, and S. Ledakowicz, *Anaerobic co-digestion of sewage sludge and organic fraction of municipal solid wastes.* Advances in Environmental Research, 2003. **7**(3): p. 609-616.

116. Boni, M.R. and L. Musmeci, *Organic fraction of municipal solid waste (OFMSW): extent of biodegradation.* Waste management & research, 1998. **16**(2): p. 103-107.

117. Veillette, M., et al., *Six month tracking of microbial growth in a metalworking fluid after system cleaning and recharging.* Annals of Occupational Hygiene, 2004. **48**(6): p. 541-546.

118. Arun R. Gavaskar, R.F.O., Jody A. Jones, *Mobile On-Site Recycling of Metalworking Fluids*. 1993: Columbus, Ohio.

119. Hijnen, W., E. Beerendonk, and G.J. Medema, *Inactivation credit of UV radiation for viruses, bacteria and protozoan (oo) cysts in water: a review.* Water research, 2006. **40**(1): p. 3-22.

120. Downes, A. and T.P. Blunt, *IV. On the influence of light upon protoplasm.* Proceedings of the Royal Society of London, 1879. **28**(190-195): p. 199-212.

121. Miller, S.L. and J.M. MacHer, *Evaluation of a methodology for quantifying the effect of room air ultraviolet germicidal irradiation on airborne bacteria.* Aerosol Science & Technology, 2000. **33**(3): p. 274-295.

122. Meulemans, C., *The basic principles of UV–disinfection of water.* 1987.

123. Johnson, D.L. and M.L. Phillips, *UV disinfection of soluble oil metalworking fluids.* AIHA Journal, 2002. **63**(2): p. 178-183.

124. Chang, S.-C., et al., *A biocide-free mineral oil nanoemulsion exhibiting strong bactericidal activity against Mycobacterium immunogenum and Pseudomonas aeruginosa.* International biodeterioration & biodegradation, 2012. **70**: p. 66-73.

125. Kirk, J., *Optics of UVB radiation in natural waters.* Ergebnisse Limnol, 1994. **43**: p. 16.

126. Swerdlow, A., et al., *Fluorescent lights, ultraviolet lamps, and risk of cutaneous melanoma.* Bmj, 1988. **297**(6649): p. 647-650.

127. Rozich, A.F. and K. Bordacs, *Use of thermophilic biological aerobic technology for industrial waste treatment.* Water Science and Technology, 2002. **46**(4-5): p. 83-89.

128. Mosleh, M., et al., *Modification of sheet metal forming fluids with dispersed nanoparticles for improved lubrication.* Wear, 2009. **267**(5-8): p. 1220-1225.

129. Samuel, J., et al., *Graphene colloidal suspensions as high performance semi-synthetic metal-working fluids.* The Journal of Physical Chemistry C, 2011. **115**(8): p. 3410-3415.

130. Manikanta, J.E., B. Srinivas, and D.S. Rao, *Effect of Nano Cutting Fluid & Process Parameters on Material Removal Rate and Surface Finish of SS304 Alloy on Turning Operation.*

131. Bakalova, T., et al., *The application potential of SiO2, TiO2 or Ag nanoparticles as fillers in machining process fluids.* Journal of cleaner production, 2017. **142**: p. 2237-2243.

132. Maynard, A.D. and E.D. Kuempel, *Airborne nanostructured particles and occupational health.* Journal of nanoparticle research, 2005. **7**(6): p. 587-614.

133. Fischer, H.C. and W.C. Chan, *Nanotoxicity: the growing need for in vivo study.* Current opinion in biotechnology, 2007. **18**(6): p. 565-571.

134. Seyedmahmoudi, S., et al., *Evaluating the use of zinc oxide and titanium dioxide nanoparticles in a metalworking fluid from a toxicological perspective.* Journal of Nanoparticle Research, 2015. **17**(2): p. 104.

APPENDIX

TREATMENTS OF MICROBIAL CONTAMINATION IN METALWORKING FLUIDS

This research has one potential application. This section, background of this application and review of the state-of-the art is provided for future reference.

A.1 Introduction

Processes using metalworking fluids (MWFs) include machining, forging, and stamping [72]. These fluids are used to provide lubrication and cooling. In 2016, the global MWF market size was valued at $9.62 billion (USD). Metalworking fluids fall under four categories: Insoluble (or straight oils), which contain 60-100% mineral oil, soluble oil (30-85% MO), semi-synthetic fluid (5-30% MO), and synthetic fluid, which contains no mineral oil and is water-based [25, 73]. These different fluids represent a trade-off in MWFs between cooling and lubrication [74]. Metalworking fluid concentration, pH levels, microbial activity, emulsion stability, corrosion susceptibility and the addition of additives vary with application and the type of fluid used [75-77].

Common Additives in Metalworking Fluids
Anti-foam
Anti-fogging
Anti-wear
Corrosion inhibitors
Extreme pressure
Odorizers/Fragrances
pH buffers
Stabilizers

Table 8: Common additives in MWFs [77]

Microbial contamination of metalworking fluids is a major problem in the industry, due to the low effectiveness and lack of options in treatment methods. Add. Contamination and the bi-products of contamination (such as sludge and organic waste) can lead to fluid, tool, and workpiece degradation. Aerosolization of the fluid and contaminants is commonplace due to the high shear forces used in metalworking [73, 78, 79]. Exposure to these contaminants can have wide-ranging and long-lasting detrimental effects on workers, including dermatitis, asthma, and hypersensitivity pneumonitis [73]. Recently, governments around the world have placed regulations on the uses of MWFs due to the exposure risks [80-82]. here other review papers on MWFs. Other literature reviews on microbial contamination, such as those by Saha et. al [75] and do not provide a detailed look into treatment mechanisms or bacterial resistance to these mechanisms. This paper presents a literature review of treatment methods of microbial contamination in metalworking fluids, with an emphasis on mechanisms of treatment.

a. Bacteria:

The fluid environment of metalworking fluids is a favorable environment for bacterial growth [83]. Fatty acids, petroleum oil, and petroleum sulfonates act as food sources for bacterial species [84]. Over 100 different species of bacteria have been observed in metalworking fluids. Both gram-positive, gram-negative and mycobacteria have been observed [75, 78, 85, 86]. High degrees of microbial loading can be present in metalworking fluids, ranging from 10^4 to 10^10 CFU/mL (colony-forming units). The types of bacteria and bacterial metabolic activity varies with the type of metalworking fluid and application. The most common genus found in MWFs is *Pseudomonads* [83]. *Pseudomonas aeruginosa, Pseudomonas fluorescens, Pseudomonas pseudoalcaligenes* are common *Pseudomonads* found in MWFs [85, 87].

Pseudomonas aeruginosa is a gram-negative bacterium with multi-drug resistance [88]. Exposure to the bacteria can lead to ventilator-associated pneumonia, sepsis syndromes, and other complications. *P. aeruginosa* has been known to form biofilms, increasing its resistance towards treatment [89].

Mycobacterium immunogenum is of particular concern in the metalworking industry. *M. immunogenum* is a non-tuberculosis causing mycobacteria. *M. immunogenum* is known to cause cancer, asthma, pulmonary infections, and of particular importance, hypersensitivity pneumonitis [76, 90-92]. Exposure to *M. immunogenum* is generally through inhalation of aerosolized bacteria. *M. immunogenum* has particularly high presence in the automotive industry [93]. This may be due to particular mix of materials and contaminants that are prevalent in the fluid in the industry, notably chromium, iron, and nickel [90]. The virulence of *M. immunogenum* is generally considered to be low compared to other species of mycobacteria (such as tuberculosis-causing mycobacteria), but the exposure and health hazards remain an issue in metalworking [94].

The co-contaminant effect seen in metalworking fluids is of particular interest. This effect takes place when multiple bacteria species are present. This combination has shown to have a mutual protective mechanism for the bacteria [95]. This mechanism may change the uptake and distribution of biocides in the cells, thereby changing the concentration and effectiveness of the treatment. Selvaraju et. al has shown that *P. fluorescens*, while in isolation has low virulence and is generally non-pathogenic, has shown to increase the biocide resistant of *M. k immunogenum*. This effect makes the study of treatment methods difficult, as testing treatment methods against particular bacterial species is not enough.

Bacteria Species	Gram	Virulence	Associated diseases	Treatment resistance	Notes
M. immunogenum	(+)	"Rapidly growing mycobacteria" but slow compared to E. coli, generally mycobacteria as a whole has low virulence	Hypersensitivity Pneumonitis, MOL (Machine Operator's Lung), cancer, asthma, pulmonary infections	Resistant to the majority of biocides – when biocides are used to kill other bacteria this gives the opportunity for mycobacteria to become the dominant flora in MWFs	Prevalent in the automotive industry, non-tuberculosis causing bacteria, no systematic reporting on infections
P. aeruginosa	(-)	Virulent but not as virulent compared to other pathogenic bacterial species (such as S. aureus)	Ventilator-associated pneumonia, sepsis syndromes	Multi-drug resistance, intrinsic and acquired mechanisms	Can infect a wide range of animal and plant hosts [38], Biofilms
P. fluorescens	(-)	Low	Generally non-pathogenic, but fevers and chills have been reported	Multi-drug resistance, intrinsic and acquired mechanisms	Foul odors, co-contaminant effect
Shewanella putrefaciens	(-)	Low	Rarely pathogenic in humans but bacteremia, soft tissue infections, and otitis media have been reported		Facultative anaerobe, foul odor (rotting fish), biofilm formation

Table 9: Predominant Bacteria in MWFs [95-100]

b. Biofilms:

Biofilms can also be a problem in metalworking fluids. Biofilms are able to share nutrients as well as protect other bacterial cells in the biofilm from harmful factors and treatment methods [101]. This shielding effect makes current treatment methods, such as biocides, and UV irradiation, less effective. Biofilms contain an abundance of bacterial species, making selective treatment, such as antibiotics, difficult [102]. Biofilms can also be resistant to cleaning and replacing of fluid [103].

Water-containing environments, such as synthetic metalworking fluids can lead to greater biofilm formation [102, 104].

c. Bacterial Detection:

Tracking the bacterial load is an important step in evaluating both the efficacy and effectiveness of treatment methods [105]. qPCR (Quantitative Polymerase Chain Reaction) is generally used to track the real-time bacterial load in metalworking fluids [90]. FISH (fluorescent in situ hybridization) [75], DGGE (Denaturing gradient gel electrophoresis) [87], FAME (fatty acid methyl ester) [106], and MTT assay (tetrazolium salt assay) [103] are also commonly used to track bacterial loads.

A.2 Treatment Methods using Biocides

Biocides can be built into the fluid as an additive or used at the end site during the cleaning and recycling process [107]. The most common treatment methods currently used are the use of biocides and cleaning and replacement of the fluid [25]. Major biocide types are displayed in Table 10. The most commonly used biocides in metalworking fluids are formaldehydes, isothiazolones, and phenols [83].

a. Biocide Mechanisms:

Bacterial growth refers to the increase in size of individual cells. Proliferation of bacteria refers to the increase in the number of cells through reproduction [25]. Biocides fall into two main categories based on their mechanisms of action – bacteriostatic and bactericidal [26]. Bacteriostatic biocides stop bacteria from reproducing and prevents the proliferation of the culture, while not necessarily killing the bacterial cells. Bactericidal biocides work by directly killing bacterial cells [27]. While at first glance bactericidal

biocides may seem superior to bacteriostatic biocides, it needs to be remembered that the success and flourishment of bacteria depends on the cultures ability to reproduce and proliferate. Due to the short life span of bacteria, bacteria cultures that cannot reproduce will die out quickly. Hence, depending on the mechanism and kinetics of the biocide, bacteriostatic biocides can be as effective as bactericidal biocides in dealing with the issue of microbial contamination in metalworking fluids [26].

Biocide Types and Mechanisms				
Biocide Types	**Notable**	**Effective against spores?**	**Mechanism**	**Notes**
Alcohols		No	Cell membrane damage, protein denaturation, metabolism interference, lysis	Not as effective at lower concentrations, used in combinations with other biocides
Aldehydes	Glutaraldehyde, **Formaldehyde**	Yes	Interaction with outer cell membrane, transport inhibition, enzyme inhibition, dehyrogenase inhibition, inhibition of RNA, DNA, and protein synthesis, lysis	
Biguanides	Chlorhexidine, **Isothiazolone**	Sporostatic	Outer and inner cell membrane damage	Rapid uptake by cells, mycobacteria highly resistant
Halogen-Releasing Agents	Chlorine-based, Iodine-based	At higher concentrations	Oxidation, disrupt protein activity; attack proteins, nucleotides, and fatty acids	
Silver Compounds		Varies	Bind to enzymes and inhibit enzyme activity, DNA interactions	
Peroxygens		At high concentrations and long contact times	Denatures proteins, oxidation with hydroxyl free radicals, affects cell permeability	Environmentally friendly
Phenols		Varies	Leakage of cell components, lysis	Cell age changes sensitivity
Bis-Phenols	Triclosan, Hexachlorophene	Sporostatic	Leakage, lysis, inhibition of cellular respiration, outer membrane permeability changes	
Quaternary Ammonium Compounds		Sporostatic	Attack cell membranes, degradation of proteins and nucleic acids	

Table 10: Biocide Types and Mechanisms [27, 95, 101]
(Most commonly used biocides in MWFs are in bold)

Biocides do not have selective toxicity, which is the process of killing microbial cells but not the host cell [108]. This is in contrast to antibiotics,

which generally have selective toxicity. Since biocides are not used as medicines (again in contrast to antibiotics), this is not as large of an issue. The lack of selective toxicity can however lead to both health and environmental issues upon exposure and is an important factor for the heavy government regulation of biocidal products. Biocides do, however, have target specificity, similar to antibiotics. Biocides are designed to attack and disrupt specific cellular mechanisms and targets. Generally antibiotics attack one target, whereas biocides generally attack several [109]. The main target sites in bacteria for biocides are the cell wall, cytoplasmic membrane, and the cytoplasm. Cell wall and membrane damage can cause leakage and lysis, leading to cell death [27]. Biocides enter the cell through diffusion or through pores in the cell wall. The method of transport for the biocide depends on the biocide size, chemical makeup, and polarity [27].

An important property to consider of biocides (and of all additives used in metalworking fluids) is the potential for interactions with other additives [25]. These interactions can be either synergistic or antagonistic. Additives will many times show low or no effect when used singularly, but when used in conjunction with other additives, a larger effect is seen. This effect makes testing the efficacy of biocides difficult, as biocides many have different effects or kinetics in the presence of different additives. This effect has been seen with combinations of coolants and biocides in metalworking fluids, and the term "biocide potentiator" was termed by Bennett [25].

b. Cons of Biocides:

Biocide Resistance:

Bacteria in metalworking fluids commonly show resistance against biocides. Bacterial resistance mechanisms can either be intrinsic or acquired [110]. Gram-negative bacteria are generally more resistance than gram-positive bacteria due to the outer membrane preventing treatment from entering

the cell. Furthermore, mycobacteria are generally more resistance to treatment than gram-negative bacteria [27]. Bacteria are generally less resistant to biocides in comparison to antibiotics. This may be due to the multi-target mechanisms used in biocides [109]. The primary intrinsic mechanisms used by bacteria is active efflux [111]. Active efflux uses active transport to move unwanted material through the cytoplasmic membrane and out of the cell. Other intrinsic mechanisms used by bacteria include the use of constitutive enzymes to degrade preservatives and biocides and spore coats. Acquired mechanisms include plasmid-mediated resistance, phenotypically-acquired resistance, and adaptations for homeostasis [110].

Biocide Regulations:

The use of biocides is heavily regulated by the EPA (Environmental Protection Agency) in the United States and the European Union [81]. The Federal Insecticide, Fungicide, and Rodenticide Act (FIFRA), and reviews of the act, notably the Federal Environmental Pesticide Control Act (FEPCA) of 1972 and the Pesticide Registration Improvement Act of 2003 (PRIA), give the EPA the authority to supervise the manufacture, sale, transport, and use of biocides in the United States [112]. New biocides must be approved for use by the EPA before use.

c. Biocide Conclusion:

The wide range of resistance mechanisms towards biocides makes biocidal treatment less effective and the development of new, successful biocides more difficult. Biocides are the most effective treatment of microbial contamination currently used in the metalworking fluid industry. However, the drawbacks to its use including inadequate effectiveness, microbial resistance, potential health and irritant problems, and regulations for use. These drawbacks show a potential need for different treatment methods.

A.3 Cleaning and Replacement of Fluid

Cleaning, recycling, and replacing metalworking fluids is another method commonly used to treat microbial contamination [113]. All metalworking fluids are designed for long term use. Cleaning can be used to remove microorganisms, as well as remove the bi-products of these organisms, such as organic waste and sludge.

a) Cleaning Mechanisms/Pros:

Different methods are used to clean water-based fluids (synthetics) versus non-water-based fluids. In water-based fluids, many additives are attracted to the workpiece or other metal surfaces in the working environment. Over time, this causes additives to be removed from the fluid environment, which slowly decreases the concentration of additives in the fluid. In addition, additives can also be degraded by microbial activity, temperature, oxidation, filtration, and evaporation. These degradation processes lead to changes in the makeup of the MWF and reduces the effectiveness of both the additives and the fluid. As the water-based fluid ages, the composition of the fluid changes leading to poorer wettability and increased surface tension, which can lead to residual mineral oil build up that is not removed by the MWF. An important method of dealing with these changes in monitoring the fluid makeup, with a focus on the concentration, pH levels, microbial contamination, conductivity, and tramp oil [114].

In non-water-based fluids, the focus is the separation of the water phase from the oil phase. Important properties to monitor in non-water-based fluids include viscosity, TBN (total base number), TAN (total acid number), flash point, contamination by solids, density, and microbial contamination (which is less common than in water-based fluids [72]) [114].

The separation of the water phase from the chemical phase can be accomplished by chemical or physical means. An acid and salt process is the traditional chemical separation that was used, however, due to regulations and new technologies, this method is no longer used in Europe or the United States [114].

Organic fraction is the current method of chemical separation that is generally used, and involves the anaerobic digestion of the organic waste [115, 116]. Methane is the main biproduct of this process. Physical separation methods include evaporation and membrane filtration [114].

b) Cons:

Replacing fluid is not ideal for multiple reasons – mainly due to high cost and difficult and heavily regulated disposal procedures. The main problems with this method of treatment is prohibitive cost and not fully removing the bacteria [117]. The bacteria cannot ever be fully removed from cleaning and replacement alone [95], and the remaining bacteria will proliferate. For example [114], consider a fluid with a microbial load of 10^7 CFU/mL. 99.9% of the fluid is removed during the cleaning process, and new fluid is added to the system. The new concentration of bacteria is 10^4 CFU/mL. This is still quite high and will quickly proliferate to the original levels of contamination. This can also lead to increased levels of biocide and treatment resistance. In addition, biofilms have shown to be resistant to fluid cleaning and replacing [75, 103].

The recycling and disposal of metalworking fluids is heavily regulated in the United States and Europe. Regulations such as the Pollution Protection Act, Toxic Substances Control Act, Resource Conservation and Recovery Act (RCRA), have brought large changes to disposal regulations in the United States. Source reduction, which is the method of reducing waste before it is created, and on-site recycling was highly encouraged on a national scale [118]. These regulations make this method of dealing with contamination costly and labor intensive and make other treatment methods (particularly those that deal with the root cause of the problem) preferable.

A.4 UV Irradiation

a) Mechanism:

Ultraviolet irradiation uses short-wavelength ultraviolet (UV-C) light to kill bacteria [119]. The wavelength of UV-C is in the range of 200-280nm [75]. This method was first described in 1879 by Downes and Blunt [120]. The radiation damages the cell DNA by destroying nucleic acids. Dimerization of both RNA and DNA prevents the replication and cellular division. This leads to cell death.

b) Pros:

This method can be used in water and in air [121]. It is commonly used in the medical community to sterilize instruments and surfaces. Many factors affect the effectiveness in its use to treat bacteria, such as the intensity and wavelength of the UV light, the time of exposure, and the intrinsic bacterial susceptibility against UV [122].

c) Cons:

In comparison to other treatment methods, UV irradiation has low antimicrobial performance [123, 124]. Exposure time is very important (usually 6-8 hours are needed for effective treatment), which can lead to UV treatment being slower than other methods. UV light is also quickly attenuated by water and other liquids. Hence, UV irradiation is only effective in shallow and clear fluids [125] and surface decontamination and is harmful to eyes and skin [126]. While use in conjunction with biocides may solve some of the issues plaguing UV treatment, high cost and lack of ease of use make the technology less preferable than other treatments.

A.5 Other Treatment Methods

a) <u>Thermophilic aerobic technology (TAT)</u>

Thermophilic aerobic technology (TAT) is a promising new treatment technology that can be used for preventing microbial contamination. While not

commonly used with MWFs, Rozich et. al have explored the use of this treatment in industrial waste [127]. TAT can reduce the bi-products of microbes in MWFs in a cost-effective and environmentally friendly way. TAT is used at the end use of the fluid, allowing the use in conjunction with cleaning and replacing the fluid while reducing the costs. The organic waste or sludge is initially sent to a thermophilic biological reactor, which digests and breaks down the waste. The waste is then sent to a solid separations system that separates the liquid waste from the solid. The liquid waste is removed from the system, while part of the solid waste returns to the thermophilic biological reactor, and the other solid waste is chemically treated before returning to the thermophilic biological reactor. The wastes are eventually converted to carbon dioxide and water. Up to 90% of organic waste and sludge can be removed using this process. A drawback to this process is that it treats the effects of microbial contamination and not the root cause. Many of the detrimental effects of contamination would still exist in the MWF, so a combination of TAT and other treatment methods would be necessary.

b) Nanotechnology

The use of technology in metalworking fluids is of high interest in current research. Much of the research has focused on improving the cooling and lubrication properties of the fluid [128-130], however a small amount of research has focused on microbial contamination. Bakalova et. al have shown that both Ag and SiO2 nanoparticles have antibacterial effects in metalworking fluids [131] while also having effects on friction and wear volume. These nanoparticles that have also shown antibacterial effects *in vitro* in other studies (need reference). The use of nanoparticles is not without drawbacks, as they can be aerosolized during the metalworking process [132] and may have toxic effects when inhaled [133, 134].

Chang et. al developed a nanoemulsion that has shown antibacterial activity against multiple bacteria species, notably *M. immunogenum* and *P.*

aeruginosa, without the use of biocides [124]. The oil droplet size of 11nm is the smallest size that had been achieved thus far in literature. Biocidal effects were evident at concentrations from 1-5% in both the short and long-term. Emulsion stability, which is generally decreased with microbial contamination, also showed improvement with this method.

The use of nanotechnology and materials in metalworking fluids is encouraging, and more research is necessary on these treatment methods, both in different types of nanoparticles and in interactions with other additives.

A.6 Conclusion

Microbial contamination of MWFs remains as a major problem in the metalworking industry. Many drawbacks for current treatment methods are evident. Biocides can be vulnerable to bacterial resistance and many times show inadequate antimicrobial performance. They also can have complex interactions with other additives, making their use difficult, and are heavily regulated due to health risks. UV irradiation has low-microbial performance compared to other methods and its energy is rapidly attenuated by liquid, making it only useful for surface decontamination and clear fluids. Biofilms are also an area of concern with UV irradiation. Cleaning and replacing fluid can be used to lower the bacterial load in MWFs, however this is expensive and is not fully effective in preventing and treating biofilms. New technologies such as thermophilic aerobic technology and the use of nanomaterials show promising potential, however more practice and research are necessary before these technologies can become widespread.